

2014

# Chemical Kinetics Analysis of Alternative Reagents for the SNCR Process

Yan Qin  
*Lehigh University*

Follow this and additional works at: <http://preserve.lehigh.edu/etd>

 Part of the [Mechanical Engineering Commons](#)

---

## Recommended Citation

Qin, Yan, "Chemical Kinetics Analysis of Alternative Reagents for the SNCR Process" (2014). *Theses and Dissertations*. Paper 1600.

This Thesis is brought to you for free and open access by Lehigh Preserve. It has been accepted for inclusion in Theses and Dissertations by an authorized administrator of Lehigh Preserve. For more information, please contact [preserve@lehigh.edu](mailto:preserve@lehigh.edu).

**Chemical Kinetics Analysis of Alternative Reagents  
for the SNCR Process**

by

Yan Qin

A Thesis

Presented to the Graduate and Research Committee

of Lehigh University

in Candidacy for the Degree of

Master of Science

in

Mechanical Engineering

Lehigh University

September 1, 2014

September 1, 2014

© Sept 1, 2014 Copyright

Yan Qin

## THESIS SIGNATURE SHEET

This thesis is accepted and approved in partial fulfillment of the requirements for the Master of Science.

---

Date

---

Dr. Carlos E. Romero,  
Thesis Advisor

---

Prof. Edward K. Levy,  
Academic Advisor

---

Prof. D. Gary Harlow,  
Chairperson of Mechanical Engineering and Mechanics Department

## **Acknowledgements**

I would like to express my gratitude to my supervisor, Dr. Carlos Romero, whose expertise, patient and unselfishness helped me considerably with my research. It would not be possible for me to finish this thesis without his vast knowledge and skills. I also would like to thank my academic advisor, Prof. Edward Levy, whose kindness and hospitality led me to Lehigh University, which was one of the best decision I ever made in my life. I appreciate his experience that ensured me to finish my graduate program smoothly. A special thanks goes to Mr. Zheng Yao, who helped me a lot at the beginning of my research and encouraged me to keep working hard when I was frustrated.

I must also acknowledge Dr. Aleksandra Milewska for her kindly suggestions and research references. My study would not be completed without her generous help.

I have to thank my family for the support and love they provided to me through my entire life.

Finally, I acknowledge my girlfriend, Meiyu, for her encouragement, patient, love and spiritual support during my entire graduate study.

## Table of Contents

|  |     |
|--|-----|
| List of Figures .....  | vii |
| List of Tables .....   | xi  |
| Abstract .....   | 1   |
| Chapter I – Introduction .....   | 2   |
| 1.1 Background .....   | 2   |
| 1.2 NO <sub>x</sub> Control Techniques for Coal-Fired Power Plants (CFPPs).....      | 4   |
| 1.2.1 NO <sub>x</sub> Formation in CFPPs .....                                       | 4   |
| 1.2.2 NO <sub>x</sub> Control Techniques for CFPPs.....                              | 4   |
| 1.3 Selective Non-Catalytic Reduction (SNCR) Technology .....                        | 6   |
| 1.3.1 SNCR Overview.....   | 6   |
| 1.3.2 Issues with SNCR Systems .....   | 7   |
| 1.4 Purpose of the Thesis .....  | 10  |
| Chapter II – Alternative Reagents for NO <sub>x</sub> Reduction in SNCR Systems..... | 12  |
| 2.1 Introduction .....   | 12  |
| 2.2 Ammonia .....  | 12  |
| 2.3 Urea .....   | 15  |
| 2.4 Cyanuric Acid.....   | 18  |
| 2.5 Monomethylamine.....   | 20  |
| 2.6 Other Reagents .....   | 21  |
| Chapter III – Chemical Kinetics Modeling of Monomethylamine for SNCRs.....           | 23  |
| 3.1 Introduction .....   | 23  |
| 3.2 Existing Monomethylamine Chemical Kinetics Models.....                           | 24  |
| 3.3 Plug Flow Reactor Modeling .....   | 29  |
| 3.4 Model Validation.....  | 32  |
| 3.5 Sensitive Analysis .....   | 37  |

|   |  |    |
|---|--|----|
| 3.5.1   | NSR Simulations .....  | 38 |
| 3.5.2   | Initial CO Concentration Simulations .....                                       | 40 |
| 3.5.3   | Initial NO Concentration Simulations .....                                       | 42 |
| 3.5.4   | Residence Time Simulations .....   | 44 |
| 3.6   | Monomethylamine Kinetics Mechanism Reduction .....                               | 46 |
| 3.7   | Simulation Comparison of Alternative Reagents for NO <sub>x</sub> Reduction..... | 53 |
| Chapter IV – Opportunities for Monomethylamine-Based SNCR in Other Industrial Applications..... |  | 57 |
| 4.1   | Introduction .....   | 57 |
| 4.2   | Gas Turbine Simulation.....  | 57 |
| Chapter V – Conclusions and Recommendations .....   |  | 67 |
| References .....  |  | 70 |
| Vita .....  |  | 77 |

## List of Figures

|  |    |
|--|----|
| <b>Figure 1.</b> US sources of NO <sub>x</sub> emissions in 2012. ....   | 3  |
| <b>Figure 2.</b> Electricity generation by fuel sources. ....  | 3  |
| <b>Figure 3.</b> Schematic of SNCR concept. ....   | 6  |
| <b>Figure 4.</b> Temperature Window of SNCR Process using ammonia at a molar ratio (NO <sub>2</sub> /NO <sub>i</sub> ) = 1.5. ....   | 9  |
| <b>Figure 5.</b> Relationship of NO <sub>x</sub> reduction rate and temperature by Azuhata et al.. Gas mixture: 100 ppm NO, 500 ppm NH <sub>3</sub> , 0 or 100 ppm H <sub>2</sub> O <sub>2</sub> , 0 ~ 15% O <sub>2</sub> . ....   | 13 |
| <b>Figure 6.</b> NO <sub>x</sub> reduction rate vs. average flue gas temperature by Lodder and Lefers. [NH <sub>3</sub> ]/[NO <sub>x</sub> ] <sub>in</sub> = 1.5, O <sub>2</sub> = 1%. (a) - No additives injected; (b) – CO injected. ....  | 14 |
| <b>Figure 7.</b> Formation of HCN from NH <sub>3</sub> and C <sub>2</sub> H <sub>6</sub> in the presence of oxygen. Conditions: 1000 vppm NH <sub>3</sub> , residual N <sub>2</sub> , τ = 0.45 sec, T = 1073 K, p = 1 bar, O <sub>2</sub> varied. Δ, 300 vppm C <sub>2</sub> H <sub>6</sub> ; □, 1500 vppm C <sub>2</sub> H <sub>6</sub> ; the dotted line is to guide the eye. .... | 15 |
| <b>Figure 8.</b> NO <sub>x</sub> reduction rate vs. temperature under different molar ratio by Jodal et al.. (a) Using ammonia as primary reductant; (b) Using urea as primary reductant. Molar ratio: □ = 0.7; ○ = 1.0; Δ = 1.3; ▲ = 1.6; X = 2.2. ....   | 16 |
| <b>Figure 9.</b> NO abatement with urea and urea + additives by Rota et al.. Inlet conditions: NO = 500ppm; urea = 600 ppm; H <sub>2</sub> O = 19%; O <sub>2</sub> = 1.7%; additive = 60 ppm; nitrogen = balance; residence time = 200/T s; P = 1 bar. ....  | 17 |
| <b>Figure 10.</b> Reaction path diagram illustrating the primary steps for nitrogen species in current RAPRENO <sub>x</sub> mechanism by Miller and Bowman. ....   | 19 |

|  |    |
|--|----|
| <b>Figure 11.</b> Experimental and numerical NO <sub>x</sub> reduction with CYA by Streichsbier et al.. The solid lines are numerical results while the dash lines represent the experimental values.....  | 19 |
| <b>Figure 12.</b> Schematic diagram of a plug flow reactor. ....   | 30 |
| <b>Figure 13.</b> Chemical kinetics modeling by implementing CHEMKIN and SENKIN. ....  | 33 |
| <b>Figure 14.</b> Comparison between experimental data by Hjuler et al. and the simulation predictions by using the mechanism by Hwang et al. for species NO and NO <sub>2</sub> . Inlet conditions: 1.0 atm; 600 K – 1200 K; residence time = 0.2 s; (in mole %) [CH <sub>3</sub> NH <sub>2</sub> ] = 0.026, [NO] = 0.0471, [O <sub>2</sub> ] = 4.0, [H <sub>2</sub> O] = 0.1, balance nitrogen. .... | 34 |
| <b>Figure 15.</b> Comparison between experimental data by Hjuler et al. and the simulation predictions by using the mechanism by Coda et al. for species NO and NO <sub>2</sub> . Inlet conditions: 1.0 atm; 600 K – 1200 K; residence time = 0.2 s; (in mole %) [CH <sub>3</sub> NH <sub>2</sub> ] = 0.026, [NO] = 0.0471, [O <sub>2</sub> ] = 4.0, [H <sub>2</sub> O] = 0.1, balance nitrogen. ....  | 35 |
| <b>Figure 16.</b> Comparison between experimental data by Hjuler et al. and the simulation predictions by using mechanism by Kantak et al. for species NO and NO <sub>2</sub> . Inlet conditions: 1.0 atm; 600 K – 1200 K; residence time = 0.2 s; (in mole %) [CH <sub>3</sub> NH <sub>2</sub> ] = 0.026, [NO] = 0.0471, [O <sub>2</sub> ] = 4.0, [H <sub>2</sub> O] = 0.1, balance nitrogen.....     | 36 |
| <b>Figure 17.</b> Comparison between experimental data by Milewska and the simulation predictions by using mechanism by Kantak et al. for outlet NO concentration. The inlet condition is varied and corresponding to different cases. The temperature slope for the simulation that is with slope is 100 K/s. ....  | 37 |

|  |    |
|--|----|
| <b>Figure 18.</b> Predicted outlet NO and NO <sub>2</sub> concentrations vs. temperature under various NSRs. ....                      | 39 |
| <b>Figure 19.</b> Predicted outlet NH <sub>3</sub> concentrations vs. temperature under various NSRs. ....                             | 39 |
| <b>Figure 20.</b> Predicted outlet HCN concentrations vs. temperature under various NSRs. ....   | 40 |
| <b>Figure 21.</b> Predicted outlet NO and NO <sub>2</sub> concentrations vs. temperature under various initial CO concentrations. .... | 41 |
| <b>Figure 22.</b> Predicted outlet NH <sub>3</sub> concentrations vs. temperature under various initial CO concentrations. ....        | 41 |
| <b>Figure 23.</b> Predicted outlet HCN concentrations vs. temperature under various initial CO concentrations. ....                    | 42 |
| <b>Figure 24.</b> Predicted outlet NO and NO <sub>2</sub> concentrations vs. temperature under various initial NO concentrations. .... | 43 |
| <b>Figure 25.</b> Predicted outlet NH <sub>3</sub> concentrations vs. temperature under various initial NO concentrations. ....        | 43 |
| <b>Figure 26.</b> Predicted outlet NH <sub>3</sub> concentrations vs. temperature under various initial NO concentrations. ....        | 44 |
| <b>Figure 27.</b> Predicted outlet NO and NO <sub>2</sub> concentrations vs. temperature under various residence times. ....           | 45 |
| <b>Figure 28.</b> Predicted outlet NH <sub>3</sub> concentrations vs. temperature under various residence times. ....                  | 45 |

|  |    |
|--|----|
| <b>Figure 29.</b> Predicted outlet HCN concentrations vs. temperature under various residence times. ....                                      | 46 |
| <b>Figure 30.</b> Further reduced mechanism tree. ....   | 52 |
| <b>Figure 31.</b> Predictions of outlet NO concentration using different reagents predicted by corresponding kinetics model. ....              | 55 |
| <b>Figure 32.</b> Predictions of outlet NO <sub>2</sub> concentration using different reagents predicted by corresponding kinetics model. .... | 55 |
| <b>Figure 33.</b> Predictions of Outlet NH <sub>3</sub> concentration using different reagents predicted by corresponding kinetics model. .... | 56 |
| <b>Figure 34.</b> Combined cycle unit diagram. ....  | 60 |
| <b>Figure 35.</b> Modeled ideal path way of flue gases. ....   | 61 |
| <b>Figure 36.</b> NO <sub>x</sub> reduction vs. temperature at various NSRs. ....  | 62 |
| <b>Figure 37.</b> NH <sub>3</sub> slip vs. temperature at various NSRs. ....   | 63 |
| <b>Figure 38.</b> HCN production vs. temperature at various NSRs. ....   | 63 |
| <b>Figure 39.</b> Unreacted MMA vs. temperature at various NSRs. ....  | 64 |

## List of Tables

|  |    |
|--|----|
| <b>Table 1.</b> Comparisons of different reagents of SNCR systems in non-experimental reactor units. ....  | 22 |
| <b>Table 2.</b> Physical properties of aqueous monomethylamine. ....   | 23 |
| <b>Table 3.</b> Higashihara et al. chemical kinetics mechanism. Units are $\text{cm}^3/(\text{mol}\cdot\text{s})$ for $A$ and $\text{cal/mol}$ for $E$ . Rate constants were expressed as $k = ATm\exp(-ERT)$ . ....   | 24 |
| <b>Table 4.</b> Hwang et al. chemical kinetics mechanism. Units are $\text{cm}^3/(\text{mol}\cdot\text{s})$ for $A$ and $\text{cal/mol}$ for $E$ . Rate constants were expressed as $k = ATm\exp(-ERT)$ . ....   | 25 |
| <b>Table 5.</b> Inlet conditions for sensitive analysis. *The underline values are the baseline conditions. ....   | 38 |
| <b>Table 6.</b> Simulation result comparison between reduced mechanism and original mechanism by Kantak et al.. Inlet condition: 1.0 atm; 700 K – 900 K; residence time = 1.0s; (in mole %) $[\text{CH}_3\text{NH}_2] = 0.01$ , $[\text{NO}] = 0.01$ , $[\text{O}_2] = 11.75$ , $[\text{H}_2\text{O}] = 9.95$ , $[\text{CO}_2] = 4.12$ , balance nitrogen. ORG – original Kantak et al.’s, RED – reduced Kantak et al.’s, $\Delta\%$ - the relative error = $ \text{ORG species} - [\text{RED species}]/[\text{ORG species}] \times 100\%$ ..... | 48 |
| <b>Table 7.</b> Reduced mechanism. Units are $\text{cm}^3/(\text{mol}\cdot\text{s})$ for $A$ and $\text{cal/mol}$ for $E$ . Rate constants were expressed as $k = ATm\exp(-ERT)$ .....   | 49 |
| <b>Table 8.</b> Further reduced mechanism. Units are $\text{cm}^3/(\text{mol}\cdot\text{s})$ for $A$ and $\text{cal/mol}$ for $E$ . Rate constants were expressed as $k = ATm\exp(-ERT)$ . ....  | 52 |
| <b>Table 9.</b> MMA consumption under best operating condition. ....   | 65 |

## **Abstract**

The objective of this thesis is to investigate alternative reagents for Selective Non-Catalytic Reduction (SNCR) of nitrogen oxides ( $\text{NO}_x$ ) for coal-fired power plants.

This thesis first reviews reported studies about available alternative reagents for SNCR  $\text{NO}_x$  reduction processes. Monomethylamine is then selected as a major subject of study, because of its superior nitrogen oxides reduction performance at temperatures under 800 K. Additionally, available chemical kinetics mechanisms for monomethylamine suited for the SNCR  $\text{NO}_x$  reduction process were modeled using the CHEMKIN software. From the chemical kinetics modeling, the detailed mechanism by Kantak et al. was selected to perform a sensitivity analysis. Two reduced mechanisms for monomethylamine are proposed. Finally, a monomethylamine-based SNCR  $\text{NO}_x$  removal system for a natural gas turbine plant was modeled and estimate of the usage of reagent in such system was calculated. The results of the simulations in this study show that the potential of monomethylamine-based SNCR  $\text{NO}_x$  reduction systems for full-scale power plants is promising and further laboratorial and field studies in this area would be valuable.

# Chapter I – Introduction

## 1.1 Background

Nitrogen oxides ( $\text{NO}_x$ ) are one of the major pollutants emitted by combustion along with other pollutants such as sulfur oxides ( $\text{SO}_x$ ) and particulate matter [1].  $\text{NO}_x$  emissions cause serious environmental problems which includes ground-level ozone, acid rain, water quality deterioration, global warming and formation of particulate matter [2]. According to 2012 data from the US Environment Protection Agency (EPA), fuel combustion was the second largest source of  $\text{NO}_x$  emissions in the US, mounting up to 33.1%. Furthermore, as shown in **Figure 1**, 16% of the  $\text{NO}_x$  emissions comes from fuel combustion for power generation. Meanwhile, despite the increasing contribution to electrical power by natural gas, due to its lower pollutant emissions and large amount of its reserves, coal is still the major fuel for power generation in the US. Coal contributed in 2013 to 1530 billion kilowatt-hour of electricity, accounting for 39% of the total electricity generation [4] (see in **Figure 2**). Coal combustion contributes to 93% of the  $\text{NO}_x$  emissions in the electricity sector [5]. Therefore, research and technology development of  $\text{NO}_x$  control technologies for coal-fired plants and other stationary sources is of great importance.

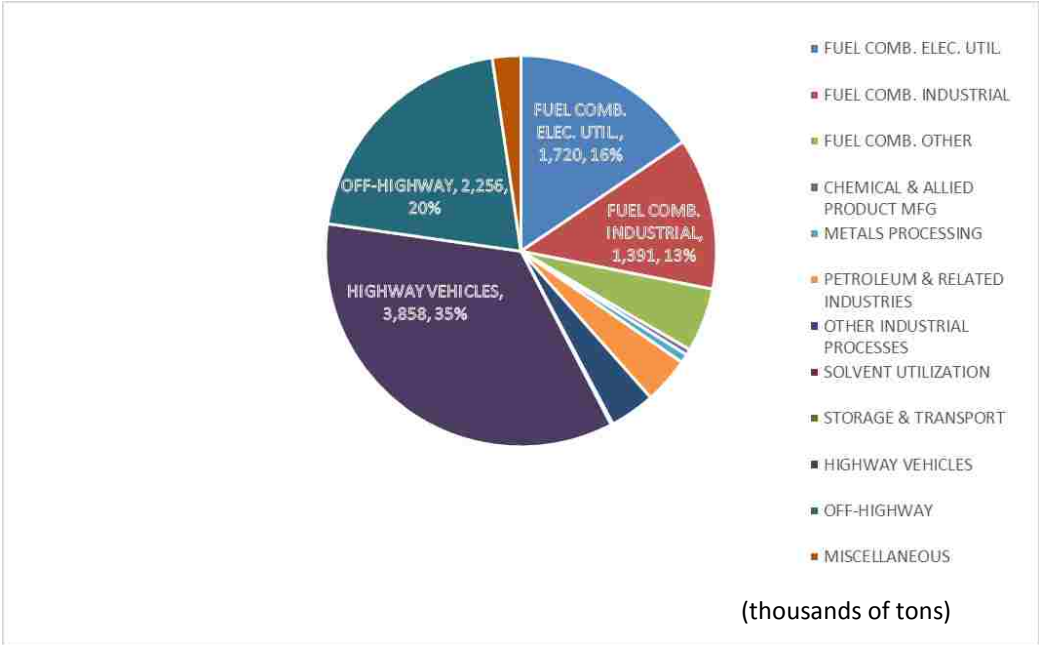


Figure 1. US sources of NO<sub>x</sub> emissions in 2012 [3].

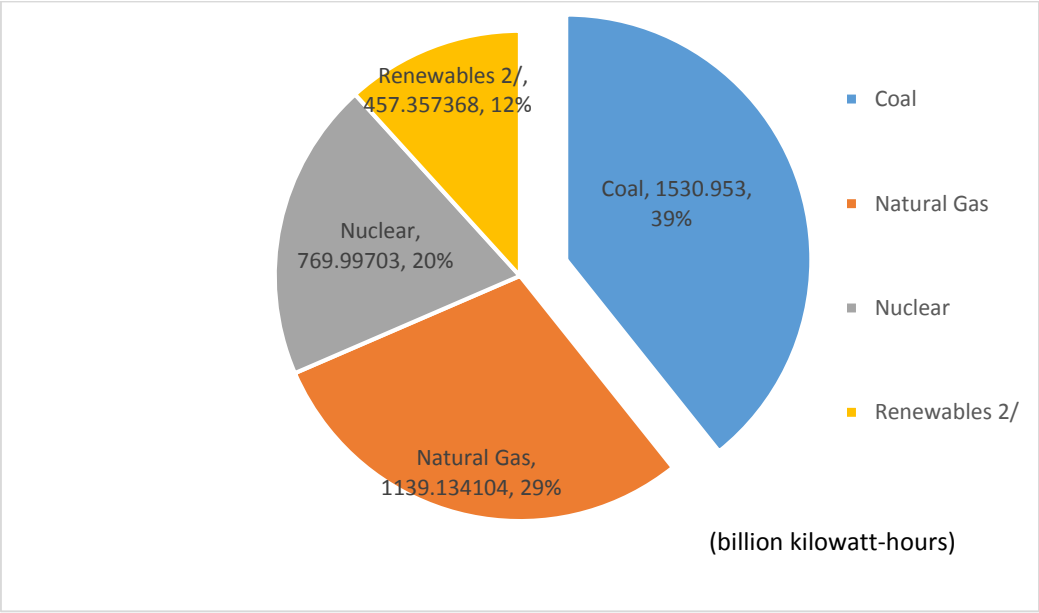


Figure 2. Electricity generation by fuel sources [4].

## **1.2 NO<sub>x</sub> Control Techniques for Coal-Fired Power Plants (CFPPs)**

### *1.2.1 NO<sub>x</sub> Formation in CFPPs*

NO<sub>x</sub> formation in CFPPs is relatively complex and understanding the mechanisms of NO<sub>x</sub> formation has led to effective development of NO<sub>x</sub> control technologies for CFPPs. NO<sub>x</sub> formed in fuel combustion processes is generally due to three different chemical mechanisms: (1) thermal fixation of nitrogen in the combustion air, which is termed “thermal NO<sub>x</sub>” [6], (2) reaction between hydrocarbon radicals and atmospheric nitrogen, which is termed “prompt NO<sub>x</sub>” [7], (3) and conversion of fuel bound nitrogen to NO<sub>x</sub> during combustion, which is referred to as “fuel NO<sub>x</sub>” [8]. Thermal NO<sub>x</sub> can mount up to 20% of the NO<sub>x</sub> emissions while the fuel NO<sub>x</sub> can contribute up to 80% [9] of the total NO<sub>x</sub> formation in CFPPs. Prompt NO<sub>x</sub> is a minor contributor to NO<sub>x</sub> production in coal-fired units. Thermal NO<sub>x</sub> can be controlled by lowering peak flame temperatures and the amount of excess air in the combustion process; meanwhile fuel NO<sub>x</sub> can be generally controlled by limiting the supply of oxygen during the initial combustion stages [1].

### *1.2.2 NO<sub>x</sub> Control Techniques for CFPPs*

There are three primary categories of NO<sub>x</sub> technologies available for NO<sub>x</sub> emissions control for CPPPs: pre-combustion control, combustion control and post-combustion control.

Pre-combustion NO<sub>x</sub> control refers to the technique that reduces the nitrogen content in the fuel or to switch to other fuels that contain lower nitrogen level. However, unlike sulfur in the coal, eliminate or reduce nitrogen species in the coal is difficult. Additionally, nitrogen is not the only parameter that has an impact on NO<sub>x</sub> formation. Other factors such

as fixed carbon, volatile matter, oxygen and moisture content also play a role in the formation of  $\text{NO}_x$  in the coal combustion process [1].

Combustion control generally includes techniques that reduce combustion temperature, oxygen availability in the primary combustion stage and modify the residence time of the combustion zone in the high temperature zones. Available technologies for combustion control of  $\text{NO}_x$  include, burner tuning, boiler optimization, excess air control, low- $\text{NO}_x$  burners, oxygen-enriched combustion, flue gas recirculation and gas reburning. These technologies are effective in reducing  $\text{NO}_x$  and used nowadays by most of the existing CFPPs. However, there are issues with them such as boiler efficiency losses, increasing the unburned carbon content in the fly ash and accelerating the rates of corrosion in the lower furnace, due to operation under a reducing atmosphere in the furnace.

Post-combustion  $\text{NO}_x$  control, also called flue gas treatment, refers to technologies that focus on removing or reducing pollutant emissions in the post-combustion gases. Most widely used post-combustion  $\text{NO}_x$  technologies are Selective Catalytic Reduction (SCR) and Selective Non-Catalytic Reduction (SNCR). SCR is one of the most common post-combustion  $\text{NO}_x$  reduction technologies employed in CFPPs, due to its high  $\text{NO}_x$  removal efficiency. SCR is associated with relatively higher retrofit costs, potential sulfur dioxide ( $\text{SO}_2$ ) to sulfur trioxide ( $\text{SO}_3$ ) conversion, catalyst deactivation and ammonia ( $\text{NH}_3$ ) slip.  $\text{NH}_3$  slip can lead to fouling of the air preheaters in CFPPS, which impacts unit availability and increase the operating and maintenance cost of the unit.

## 1.3 Selective Non-Catalytic Reduction (SNCR) Technology

### 1.3.1 SNCR Overview

$\text{NO}_x$  reduction by SNCR, or SNCR De- $\text{NO}_x$ , is a technology that consists of injecting chemical reagents (usually at a location where the temperature is in the active reagent reaction temperature range), which mix thoroughly with the flue gases containing  $\text{NO}_x$ . The  $\text{NO}_x$  is removed by chemical reactions between the reagent and the  $\text{NO}_x$  in the flue gas. A schematic of the general SNCR concept is shown in **Figure 3**.

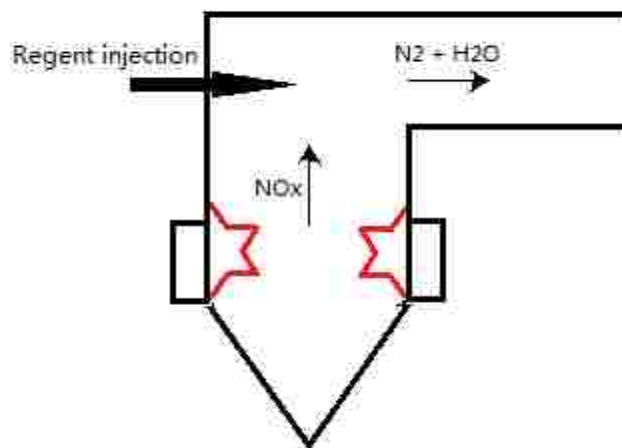
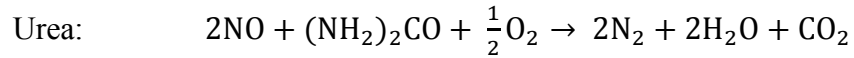


**Figure 3.** Schematic of SNCR concept.

Most commonly used reducing SNCR reagents for full-scale applications include ammonia, ( $\text{NH}_3$ ), (introduced by Exxon Research & Engineering Co. [10] in 1975) and urea, ( $\text{CO}(\text{NH}_2)_2$ ), (patented by Arand et al. [11] in 1980). These reagents require a reaction

temperature window between 1125 K and 1450 K [12]. The assumed global NH<sub>3</sub> and urea SNCR chemical reactions are presented below [1]:



Reported studies show that the performance of SNCR system can theoretically be affected by the following factors: injection point temperature and cumulative residence time, oxygen content of the flue gas, sulfur content in the fuel, untreated NO concentration in the flue gas, and moisture concentration and carbon monoxide (CO) content of the flue gas. Additionally, due to the sensitivity of the SNCR process to the boiler process conditions, to achieve greatest NO<sub>x</sub> removal effectiveness, the SNCR is also highly dependent on the flue gas temperature window at the reagent injection zone, flue gas residence time in the active temperature range, the normalized stoichiometric ratio between the reagent and NO<sub>x</sub>, and mixing between the reagent and the flue gas. These factors are important to maximize the NO<sub>x</sub> reduction performance of SNCR systems in full-scale applications [13].

### *1.3.2 Issues with SNCR Systems*

Most critical issues with current SNCR systems are related to the narrow active temperature window and potential NH<sub>3</sub> slip. Theoretically, NH<sub>3</sub>-based and urea-based SNCR systems can achieve as high as 70-80% of NO<sub>x</sub> reduction under ideal process conditions; however, 35% to 50% abatement is typically achieved in large full-scale power plants.

The optimal reduction temperature for the SNCR technology is around 1235 K for  $\text{NH}_3$ , with an effective temperature window between 1175 K – 1275 K (Poole and Graven [14] and Wise and Frech [15]), as shown in **Figure 4**. Below the optimal temperature, the  $\text{NO}_x$  reduction rate is limited by insufficient hydroxide ( $[\text{OH}]$ ) and oxygen ( $[\text{O}]$ ) radical concentrations and slows down the kinetics rates [14]. At temperatures below the optimal level, the amount of unreacted  $\text{NH}_3$  increases. At temperatures higher than the optimal level, the  $\text{NH}_3$  starts to react with  $\text{O}_2$  rather than with  $\text{NO}$  leading to increased  $\text{NO}_x$  formation. Many studies have been carried out on shifting the optimal reduction temperature to lower levels and widening the reduction temperature window. By adding additives, the  $\text{NO}_x$  reduction rate by  $\text{NH}_3$  and urea SNCR system can be improved. For example, Lee et al. [16] reported that by adding alkalines as additives to an urea-based SNCR system, more than 30% additional  $\text{NO}_x$  reduction improvement can be achieved.

Muzio et al. [17] reported a study on monomethylamine ( $\text{CH}_3\text{NH}_2$ ), dimethylamine ( $(\text{CH}_3)_2\text{NH}$ ) and trimethylamine ( $(\text{CH}_3)_3\text{N}$ ) as substitutes for  $\text{NH}_3$  injection. Research with hydrazine ( $\text{N}_2\text{H}_4$ ) was carried out by Azuhata et al. [18] and the result showed that a lower optimal temperature (from 775 K to 875 K) was achieved by injecting  $\text{N}_2\text{H}_4$  at low oxygen conditions. Wenli et al. [19] studied widening the temperature window of the SNCR and their experiments showed that several additives, including monomethylamine ( $\text{CH}_3\text{NH}_2$ ), can greatly lower the temperature window, achieving an 800 K optimal temperature window. Bae et al. [20] also found that adding  $\text{CO}$  or  $\text{CH}_4$  can successfully lower the optimal SNCR temperatures and widen the effective temperature window. These mentioned researches indicate that there is a major interest and there are opportunities to

improve the SNCR temperature situation by using additives. This is also true for alternative reagents, which can be used as substitutes to  $\text{NH}_3$  and urea.

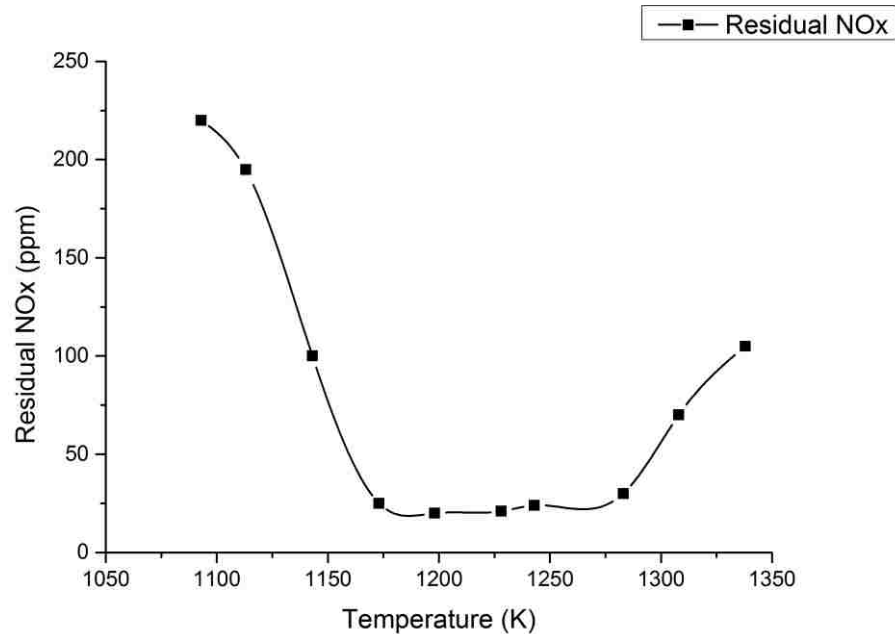


**Figure 4.** Temperature Window of SNCR Process using ammonia at a molar ratio ( $\text{NO}_2/\text{NO}_1$ ) = 1.5 [21].

The resulting  $\text{NH}_3$  from SNCRs is also considered an air pollutant in industrial applications. Unreacted  $\text{NH}_3$  emissions, which is also termed ammonia slip, is a key factor that reflects the performance of the  $\text{NO}_x$  reduction system along with the reagent consumption and  $\text{NO}_x$  reduction rate. The unreacted  $\text{NH}_3$  can lead to: (1) ammonium salts formation which usually include ammonia bisulfate ( $\text{NH}_4\text{HSO}_4$ ), a salt that causes fouling of air preheaters and other downstream surfaces in boilers; (2) ammonium chloride plume from the stack; (3) ammonia odor from the fly ash; and (4) gaseous ammonia emission, if the level of the slip is high because of poorly SNCR control. Since ammonium bisulfate is extremely sticky and corrosive, the formation of it causes serious problems to the boiler back-end combustion equipment and contribute to fouling and plugging [22]. As stated

previously, high levels of  $\text{NH}_3$  slip can occur when the reaction temperature is on the left side of the SNCR temperature window and such situation is usually aggravated by improper reagent injection, poor mixing between reagent and flue gas and insufficient residence time for reagent and flue gas staying at the desired temperature range. Moreover, unsteady boiler operating conditions can also contribute to the reagent and flue gas reacting outside the temperature window even if the SNCR system is well-designed, resulting in high levels of  $\text{NH}_3$  slip. All this indicates again the need of additives and alternative SNCR reagents, which would not suffer from the  $\text{NH}_3$  slip problems associated with conventional SNCR systems.

Despite the mentioned issues of the SNCR technology, it is still considered a cost-effective post-combustion  $\text{NO}_x$  reduction technique, because of its relatively simple retrofit, and low capital and operating cost, as compared to other  $\text{NO}_x$  reduction technologies for existing coal-fired utility boilers.

## **1.4 Purpose of the Thesis**

The main purpose of the research performed for this thesis was to study alternative reducing reagents for the SNCR De- $\text{NO}_x$  system, which are capable of being effective at lower flue gas temperatures, with a wider temperature window and lower or negligible  $\text{NH}_3$  slip. The research focused particularly on studying the chemical kinetics mechanism of an alternative reagent, monomethylamine (MMA) or also known as methylamine, for  $\text{NO}_x$  reduction by SNCR systems. MMA was chosen due to its indicated performance at comparatively low temperatures. An additional goal of this study is to propose a reduced MMA-based SNCR  $\text{NO}_x$  reduction kinetics mechanism for modeling of SNCR systems,

which has a good agreement with available experimental data. A reduced mechanism could then be used to simulate the performance of a MMA-based SNCR system, which would justify the benefit from alternative reagents. Research on chemical kinetics modeling of alternative reagents for the SNCR NO<sub>x</sub> removal process provides a good tool for SNCR systems analysis and it also broadens the application of the SNCR technology to other industrial applications that can possibly lead to new markets.

# Chapter II – Alternative Reagents for NO<sub>x</sub> Reduction in SNCR Systems

## 2.1 Introduction

There are different reagents for SNCR systems, which have a range of performances and different impact on the NO<sub>x</sub> reduction process. The most currently used reagents for coal-fired power plant applications are NH<sub>3</sub> and urea. However, other alternative SNCR reagents have been studied and experimented in either laboratory or small-scale units. This chapter provides a literature review of reagents that have been studied and their indicated industrial applications.

## 2.2 Ammonia

As a NO<sub>x</sub> reduction reagent for SNCR systems in CFPPs, NH<sub>3</sub> was first introduced and studied in 1975 by Exxon Research & Engineering Co. [10]. Since then, many studies have been carried out in order to improve the performance of NH<sub>3</sub>-based SNCR systems. Generally, improvements are obtained by adding other chemicals as additives, mixed with NH<sub>3</sub>. In 1975, Lyon [10] stated that the addition of hydrogen can effectively reduce the optimal temperature at which NH<sub>3</sub> and flue gas react, NO<sub>x</sub> reduction is enhanced and NH<sub>3</sub> slip is reduced at temperatures lower than the typical optimal temperatures. Data collected by Muzio et al. [23, 24] confirmed that even small quantities of hydrogen addition can provide significant improvement over the solely NH<sub>3</sub>-based SNCR. In another study, Azuhata et al. [25] reported 90% NO<sub>x</sub> reduction in experiments in a Pyrex flow reactor at 825 K at different O<sub>2</sub> levels by injecting hydrogen peroxide (H<sub>2</sub>O<sub>2</sub>). **Figure 5** shows result

from that research where  $H_2O_2/NO$  ratios as low as 1.0 were enough to shift the SNCR temperature window by approximately 300 K.

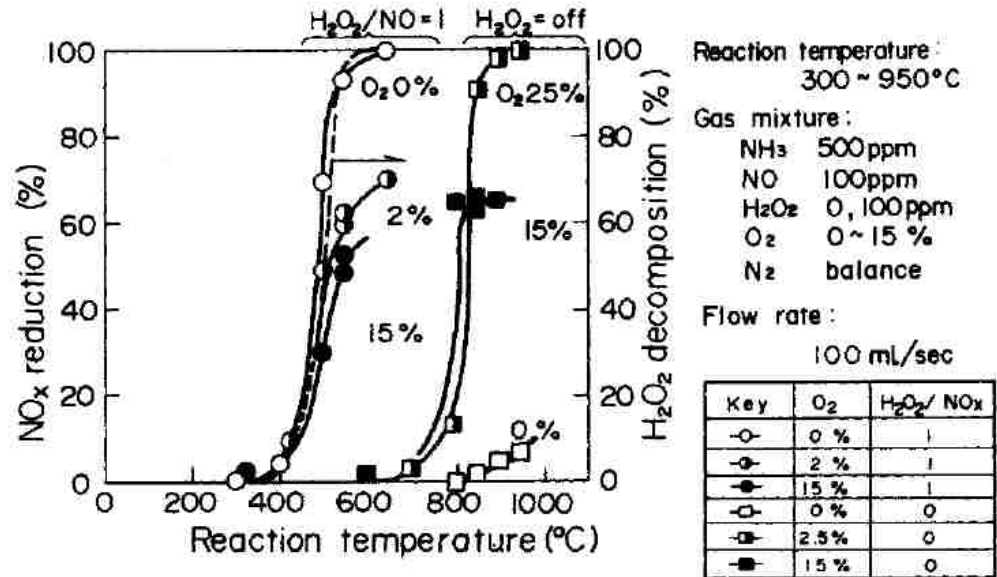


**Figure 5.** Relationship of NO<sub>x</sub> reduction rate and temperature by Azuhata et al. [25]. Gas mixture: 100 ppm NO, 500 ppm NH<sub>3</sub>, 0 or 100 ppm H<sub>2</sub>O<sub>2</sub>, 0 ~ 15% O<sub>2</sub>.

Lodder and Lefers [26] reported that by injecting natural gas, ethane (C<sub>2</sub>H<sub>6</sub>) and carbon monoxide along with NH<sub>3</sub> can decrease the optimal reaction temperature by 150 K – 200 K while achieving up to 75% NO<sub>x</sub> removal efficiency, see **Figure 6**.

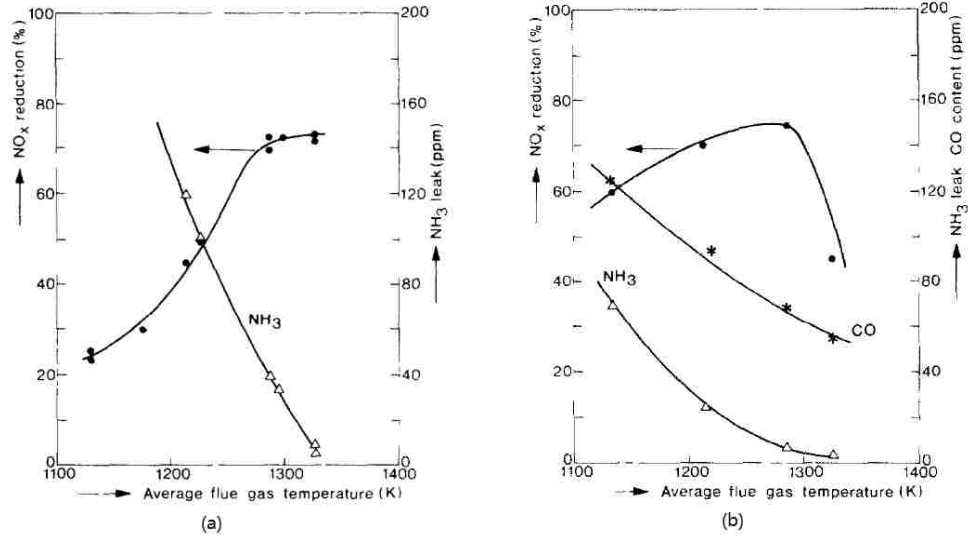


**Figure 6.** NO<sub>x</sub> reduction rate vs. average flue gas temperature by Lodder and Lefers [26].  $[\text{NH}_3]/[\text{NO}_x]_{\text{in}} = 1.5$ ,  $\text{O}_2 = 1\%$ . (a) - No additives injected; (b) – CO injected.

Wenli et al. [27] conducted studies on improving the NH<sub>3</sub>-based SNCR performance by adding a hydrocarbon, such as methane (CH<sub>4</sub>), ethane (C<sub>2</sub>H<sub>6</sub>), butane (C<sub>4</sub>H<sub>10</sub>) or ethylene (C<sub>2</sub>H<sub>4</sub>). The results showed that the temperature window can be downward shifted while achieving greater than 75% NO<sub>x</sub> removal efficiencies. Other work by Leckner et al. [28] found very little effectiveness of hydrogen, methane, ethane and butane for SNCR enhancement under specific conditions in circulating fluidized bed boilers.

Besides the mentioned studies on additives, researches have also focused on lowering or eliminating NH<sub>3</sub> slip from the SNCR process. Robin et al. [29] reported that NH<sub>3</sub> slip can be dramatically reduced by adding CH<sub>4</sub> at 1120 K with minor impact on NO<sub>x</sub> emissions reduction, with the NH<sub>3</sub> slip limited to below 10 ppm, at a CH<sub>4</sub> to NH<sub>3</sub> ratio of 2.4. An investigation carried out by Teixeira et al. [30-32] indicated that a decrement in NH<sub>3</sub> slip can result from an increment in gas CO level. NH<sub>3</sub> slips of less than 5 ppm, over a temperature range from 1025 K to 1350 K, was achieved when the initial CO concentration was 2000 ppm. Hemberger et al. [33] experimentally and numerically

studied the effect of hydrocarbon additives on  $\text{NH}_3$  slip, the results showed that in the presence of additives,  $\text{NH}_3$  emissions are much less than without additives. The  $\text{NH}_3$  slip was below the 5 ppm detection limit with a 200 ppm hydrocarbon level and  $\text{NH}_3/\text{NO}_i = 1.5$ . However, these researchers also reported that when additives were added, large amounts of HCN were produced, which was up to 300 ppm, as shown in **Figure 7**.

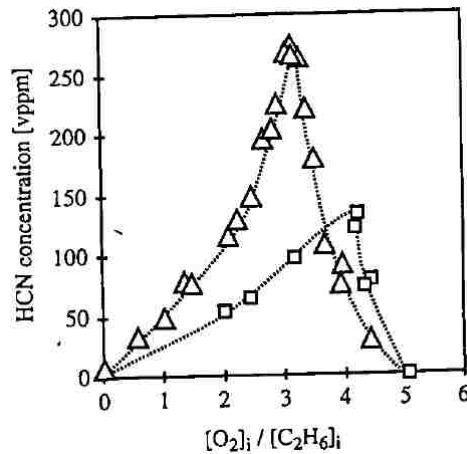


**Figure 7.** Formation of HCN from  $\text{NH}_3$  and  $\text{C}_2\text{H}_6$  in the presence of oxygen [33]. Conditions: 1000 vppm  $\text{NH}_3$ , residual  $\text{N}_2$ ,  $\tau = 0.45$  sec,  $T = 1073$  K,  $p = 1$  bar,  $\text{O}_2$  varied.  $\Delta$ , 300 vppm  $\text{C}_2\text{H}_6$ ;  $\square$ , 1500 vppm  $\text{C}_2\text{H}_6$ ; the dotted line is to guide the eye.

The major advantages of using ammonia as a reagent in SNCR systems are that it is a highly-mature technology and its relatively cost-effective. However, it has many associated drawbacks, such as low  $\text{NO}_x$  reduction rate at low temperatures, higher  $\text{NH}_3$  slip at required  $\text{NO}_x$  reduction rates, handling difficulty and high toxicity.

### 2.3 Urea

Urea was first studied as an alternative reagent to  $\text{NH}_3$  in 1980 by Salimian and Hanson [34]. They found that the maximum  $\text{NO}$  removal rate by urea was comparable to that of  $\text{NH}_3$  injection while the temperature window for urea was lower than that for  $\text{NH}_3$ . Arand

et al. [11] reported that the urea-based SNCR could achieve as high as 70% NO<sub>x</sub> reduction at temperatures in the range from 1290 K to 1330 K in a natural gas fired furnace. Chen et al. [35] conducted experimental studies in a tunnel furnace simulating the thermal environment of pulverized coal boilers and the results showed that around 45%-50% of NO was removed at optimal temperatures around 1273 K. Jodal et al. [36] carried out experiments with NH<sub>3</sub> and urea in a pilot-scale reactor. Their results included in **Figure 8** indicate that the temperature window for urea and NH<sub>3</sub> is similar; however, the peak NO<sub>x</sub> reduction was larger with urea than that with NH<sub>3</sub>, and the temperature for maximum NO<sub>x</sub> removal was shifted upward by 50K.

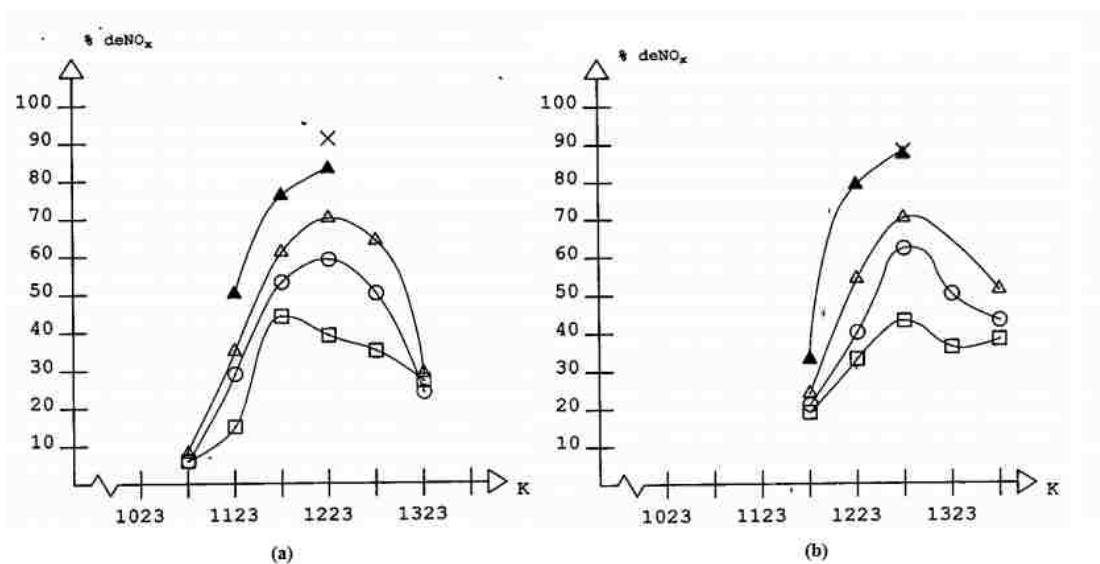


**Figure 8.** NO<sub>x</sub> reduction rate vs. temperature under different molar ratio by Jodal et al. [36]. (a) Using ammonia as primary reductant; (b) Using urea as primary reductant. Molar ratio: □ = 0.7; ○ = 1.0; △ = 1.3; ▲ = 1.6; X = 2.2.

A test of NO<sub>x</sub> removal using urea injection at the KVA Bessel Municipal Incineration Solid Waste Plant was performed by Jones et al. [37]. A 65% NO reduction was achieved at temperatures between 1220 K and 1270 K, while the NH<sub>3</sub> slip was less than 5 ppm. The effect of urea molar ratio and reaction temperature on NO abatement in a pilot-scale flow

reactor was studied by Lee and Kim [38] with good success. Similar to  $\text{NH}_3$  injection, the performance of the urea-based SNCR  $\text{NO}_x$  reduction can be affected by additives. Teixeira et al. [32] investigated the impact of several additives, which include methane, different combinations of hydrocarbons, carbon monoxide, ethylene glycol, hexa-methyl tetra-amine and furfural, on urea-based  $\text{NO}_x$  reduction efficiency. The results indicate that the  $\text{NO}_x$  reduction efficiency is very sensitive to the additive injection rates, mainly resulting in a noticeable downward reaction temperature window shift. The effect of oxygenated additives such as esters, phenols, carboxylic acids, aldehydes, ethers and alcohols on the urea-based SNCR  $\text{NO}_x$  process was studied by Rota and Zanoelo [39] in 2003 (see **Figure 9**). According to the results from an experimental reactor, all the species studied in the reactor were capable of widening the urea reaction temperature window while maintaining peak  $\text{NO}_x$  removal efficiencies.

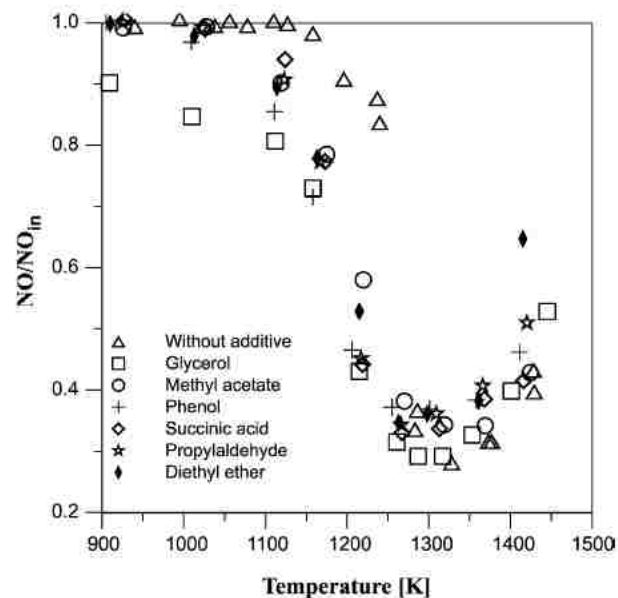


**Figure 9.** NO abatement with urea and urea + additives by Rota et al. [39]. Inlet conditions:  $\text{NO} = 500\text{ppm}$ ; urea = 600 ppm;  $\text{H}_2\text{O} = 19\%$ ;  $\text{O}_2 = 1.7\%$ ; additive = 60 ppm; nitrogen = balance; residence time =  $200/T$  s;  $P = 1$  bar.

Known problems of using urea in SNCR systems include formation of additional nitrous oxide ( $\text{N}_2\text{O}$ ) and carbon monoxide emissions [37]. Additionally, the risk of fouling and corrosion at the boiler back-end is greater when using urea as a reagent in SNCR systems. It should be noticed that urea as a reductant in SNCR systems has some advantages, such as ease of reagent handling, since urea is a non-hazardous, stable, non-explosive and non-flammable chemical.

## 2.4 Cyanuric Acid

Cyanuric acid ( $(\text{CNOH})_3$ ) was initially studied as a  $\text{NO}_x$  reduction reagent in 1986 by Perry and Siebers [40]. They experimentally investigated the cyanuric acid (CYA) reduction process in a flow reactor with simulated exhaust gas and the exhaust gas from a diesel engine. The results showed CYA has a better performance in  $\text{NO}_x$  reduction than  $\text{NH}_3$  at high  $\text{O}_2$  and  $\text{CO}$  concentrations in the exhaust gas. The commercial process that uses CYA as a reagent to reduce  $\text{NO}_x$  in flue gases is termed RAPRENO $_x$  and it was patented in 1988 by Perry [41]. Caton and Siebers [42] compared the  $\text{NO}$  removal by CYA with that by  $\text{NH}_3$  and suggested that CYA and  $\text{NH}_3$  have different reduction processes according to the experimental results. Miller and Bowman [43] performed modeling studies on the chemical mechanism of the CYA-based  $\text{NO}_x$  reduction process. The proposed chemical mechanism of the process is shown in **Figure 10**. Streichsbier et al. [44] investigated a technique which uses CYA as a  $\text{NO}_x$  reduction reagent and was able to obtain up to 85%  $\text{NO}_x$  reduction at temperatures between 970 K and 1070 K (see **Figure 11**).

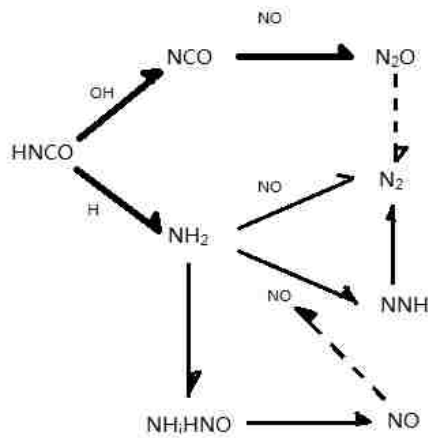


**Figure 10.** Reaction path diagram illustrating the primary steps for nitrogen species in current RAPRENOx mechanism by Miller and Bowman [44].

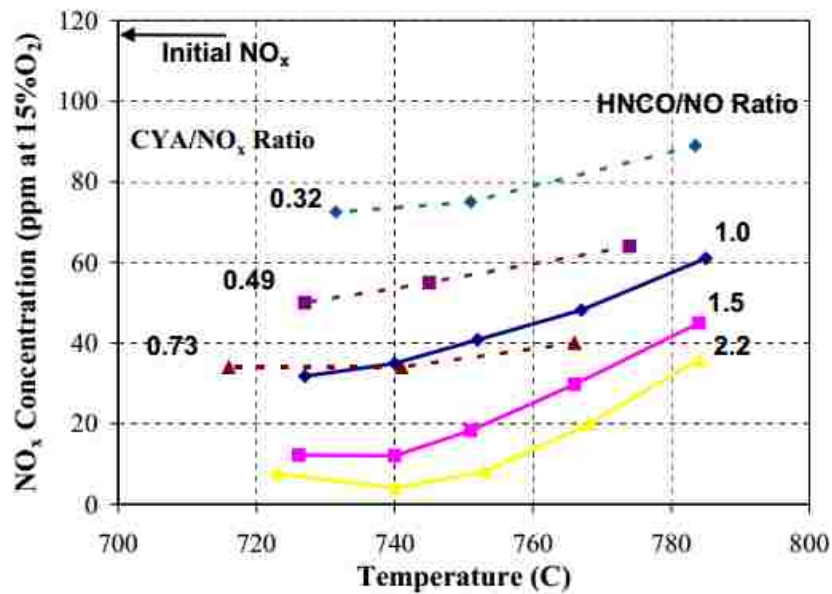
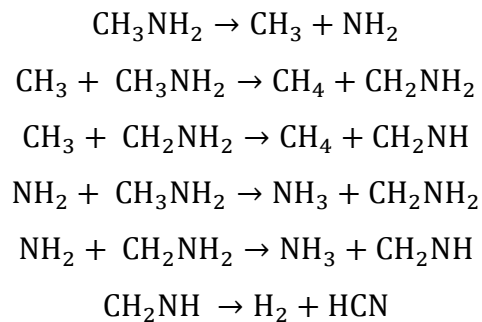


**Figure 11.** Experimental and numerical NO<sub>x</sub> reduction with CYA by Streichsbier et al. [44]. The solid lines are numerical results while the dash lines represent the experimental values.

The major advantages of using CYA as a NO<sub>x</sub> reduction reagent are the absence of unreacted ammonia in the flue gases, high efficiency and its relatively low cost. However, the CYA-based process does suffer of problem of potential N<sub>2</sub>O emissions.

## 2.5 Monomethylamine

Early studies on methylamine or monomethylamine (MMA) by Jolley [45] and Emeleus [46] indicated that MMA can be thermally decomposed to H<sub>2</sub>, hydrogen cyanide (HCN), CH<sub>4</sub> and NH<sub>3</sub> at temperatures in the range between 830 K and 950 K. Later, Dorko et al. [47] studied the thermal decomposition of MMA in a shock tube at temperatures ranging from 1275 K to 2400 K and a decomposition mechanism was proposed as below:



Wenli et al. [19] conducted an experimental investigation aiming at widening the temperature window of the SNCR NO<sub>x</sub> removal process and studied the behavior of MMA, both as a reagent and an additive. The data from their laboratory experiments indicate that MMA is capable of achieving significant NO reductions at temperatures as low as 800 K, with a comparatively wide reaction temperature window. The use of MMA as reagent in SNCR NO<sub>x</sub> reduction systems was also studied by Yoshihara et al. [48] and Nakanishi et al. [49]. They applied MMA to a proposed SNCR system for diesel engines [50]. The experimental results showed that up to 80% of NO<sub>x</sub> removal can be obtained at system temperatures in the range between 690 K and 715 K. The results were confirmed by Xu et al. [51] using an actual engine equipped with an experimental SNCR system, with 40% MMA aqueous solution injection. Additionally, Milewska et al. [52] tested a laboratory scale MMA-based SNCR NO<sub>x</sub> reduction setup, with highest NO<sub>x</sub> removal efficiencies

obtained at temperatures between 735 K and 750 K, with relatively long residence times, above 3 seconds. However, high HCN emissions were detected in the tests which could be considered as a major drawback of a MMA-based SNCR NO<sub>x</sub> control system. Available literature and experimental results on the potential application of MMA for NO<sub>x</sub> emissions reduction in coal-fired boilers are still lacking. However, bench-scale studies and the experiments on diesel engines do provide a promising possibility of using MMA as a reagent in SNCR NO<sub>x</sub> reduction systems for coal-fired boilers. Furthermore, an appropriate, validated, detailed chemical kinetics model that would provide reasonable predicting capabilities is of great interest.

## 2.6 Other Reagents

Some other novel reagents for the SNCR NO<sub>x</sub> reduction process have been studied by many researchers. Chen et al. [35] conducted both experimental and kinetic modeling studies on NO<sub>x</sub> reduction by –NH and –CN compounds, which included (HOCN)<sub>3</sub>, CO(NH<sub>2</sub>)<sub>2</sub> and ammonium sulfate. Among the reagents studied, ammonium sulfate showed superior performance as a NO reducing reagent, compared to traditional reagents such as urea and CYA; however, the extra SO<sub>2</sub> production might be a drawback for actual industrial application. Mahmood et al. [53] performed experiments on the performance of ammonium carbonate for NO<sub>x</sub> removal and achieved a 32% NO<sub>x</sub> reduction efficiency at about 1150 K. Wenli et al. [19] investigated the use of ethylenediamine (CH<sub>2</sub>NH<sub>2</sub>)<sub>2</sub> as a reagent for the SNCR NO<sub>x</sub> reduction processes and reported that (CH<sub>2</sub>NH<sub>2</sub>)<sub>2</sub> starts to react with NO at temperature around 925 K and gets a wider temperature window at about 1110 K.

**Table 1** shows a comparisons between different reagents regarding their NO<sub>x</sub> reduction performance. Although, researches have succeeded in widening the SNCR active temperature window or enhancing the removal efficiency of commercial SNCR systems by using alternative reagents, one alternative reagent, MMA seems to provide an interesting option to the traditional NH<sub>3</sub>- and urea-based SNCR systems. The NO removal efficiency and the low optimal reaction temperatures of MMA are the main advantages seen from a MMA-based process which can perform at temperatures below 900 K. This warrant a further study of MMA for SNCR applications.

**Table 1.** Comparisons of different regents of SNCR systems in non-experimental reactor units.

| Regent          | Optimal Temperature Range | Typical/ Reported peak NO <sub>x</sub> Reduction Rate | NH <sub>3</sub> Slip | Disadvantages  |
|-----------------|---------------------------|---|----------------------|--|
| NH <sub>3</sub> | 1000 K – 1200 K           | 50% – 70%   | ≤5 ppm               | <ul style="list-style-type: none"> <li>• Not active at temperatures below 800 K;</li> <li>• Toxic</li> </ul>   |
| Urea            | 1220 K – 1330 K           | 45% – 67%   | ≤5 ppm               | <ul style="list-style-type: none"> <li>• Additional nitrous oxide and carbon monoxide emissions;</li> <li>• Greater chances of fouling and corrosion;</li> <li>• Not active at temperatures below 800 K</li> </ul> |
| CYA             | 970 K – 1340 K            | 60% – 80%   | ≤5 ppm               | <ul style="list-style-type: none"> <li>• Additional nitrous oxide emissions;</li> <li>• Not active at temperatures below 800 K</li> </ul>  |
| MMA             | 690 K – 800 K             | Up to 80%   | ≤5 ppm               | <ul style="list-style-type: none"> <li>• HCN emissions</li> </ul>  |

## Chapter III – Chemical Kinetics Modeling of

### Monomethylamine for SNCRs

#### 3.1 Introduction

Monomethylamine is a colorless, flammable, corrosive and toxic gas with strong odor. It is usually used as an aqueous solution and stored in well-ventilated systems [54]. The physical properties of aqueous methylamine are listed in **Table 2**.

**Table 2.** Physical properties of aqueous monomethylamine [55].

| Aqueous Monomethylamine                 |         |         |
|---|---------|---------|
| Property                                | 40% MMA | 50% MMA |
| Boiling point (K)                       | 316     | 304     |
| Freezing Point (K)                      | 235     | 227     |
| Density (liquid) at 298 K (g/ml)        | 0.897   | 0.880   |
| Vapor pressure at 298 K (kPa)           | 50      | 76      |
| Flash point, Closed cup (ASTM D-92) (K) | 261     | 239     |

MMA has shown the promise of better performance as an SNCR NO<sub>x</sub> reduction reagent than traditional chemicals like NH<sub>3</sub>, urea and CYA, due to its low optimal temperature range (below 950 K) and comparatively low NH<sub>3</sub> slip [50]. This chapter focuses on reviewing available kinetics models of MMA – NO<sub>x</sub> reactions and reports a reduced chemical kinetics scheme for the MMA SNCR NO<sub>x</sub> reduction process. It also reports comparisons with other alternative reagents in order to evaluate the advantages of using MMA for the SNCR process over other chemicals. Chemical kinetic simulations were performed using the CHEMKIN software, under plug flow reactor conditions.

### 3.2 Existing Monomethylamine Chemical Kinetics Models

Early studies of MMA kinetics mainly focused on the reactions that take place at high temperatures. Higashihara et al. [56] in 1987 proposed a chemical kinetics mechanism of MMA thermal decomposition valid in a temperature range from 1436 K to 1820 K. The mechanism consists of 18 species and 28 reactions and satisfactorily agrees with experimental results obtained by using laser kinetic absorption spectroscopy behind reflected shock waves in a shock tube. The Higashihara's mechanism is listed in **Table 3**.

**Table 3.** Higashihara et al. [56] chemical kinetics mechanism. Units are  $\text{cm}^3/(\text{mol}\cdot\text{s})$  for  $A$  and  $\text{cal/mol}$  for  $E$ . Rate constants were expressed as  $k = AT^m \exp(-E/RT)$ .

| Reaction  | $A$      | $m$ | $E$   |
|---|----------|-----|-------|
| 1. $\text{CH}_3\text{NH}_2 + \text{M} = \text{CH}_3 + \text{NH}_2 + \text{M}$         | 4.80E+17 | 0   | 62618 |
| 2. $\text{CH}_3\text{NH}_2 + \text{M} = \text{CH}_2\text{NH}_2 + \text{H} + \text{M}$ | 2.00E+17 | 0   | 88430 |
| 3. $\text{CH}_3 + \text{CH}_3\text{NH}_2 = \text{CH}_4 + \text{CH}_2\text{NH}_2$      | 5.50E-01 | 4   | 8365  |
| 4. $\text{NH}_2 + \text{CH}_3\text{NH}_2 = \text{NH}_3 + \text{CH}_2\text{NH}_2$      | 1.30E+14 | 0   | 20076 |
| 5. $\text{H} + \text{CH}_3\text{NH}_2 = \text{H}_2 + \text{CH}_2\text{NH}_2$          | 5.50E+12 | 0   | 3107  |
| 6. $\text{CH}_2\text{NH}_2 = \text{H} + \text{H}_2\text{CNH}$                         | 1.50E+11 | 0   | 39913 |
| 7. $\text{H} + \text{CH}_2\text{NH}_2 = \text{H}_2 + \text{H}_2\text{CNH}$            | 1.00E+13 | 0   | 0     |
| 8. $\text{H} + \text{CH}_2\text{NH}_2 = \text{CH}_3 + \text{NH}_2$                    | 1.00E+13 | 0   | 0     |
| 9. $\text{H} + \text{H}_2\text{CNH} = \text{H}_2 + \text{HCNH}$                       | 1.50E+14 | 0   | 10038 |
| 10. $\text{H} + \text{HCNH} = \text{H}_2 + \text{HCN}$                                | 2.00E+13 | 0   | 0     |
| 11. $\text{HCNH} + \text{M} = \text{H} + \text{HCN} + \text{M}$                       | 3.00E+15 | 0   | 32026 |
| 12. $\text{H}_2\text{CNH} + \text{M} = \text{H}_2 + \text{HCN} + \text{M}$            | 1.00E+09 | 0   | 0     |
| 13. $\text{H}_2 + \text{CN} = \text{H} + \text{HCN}$                                  | 7.50E+13 | 0   | 0     |
| 14. $\text{NH}_3 + \text{M} = \text{NH}_2 + \text{H} + \text{M}$                      | 2.50E+16 | 0   | 93688 |
| 15. $\text{NH}_3 + \text{H} = \text{NH}_2 + \text{H}_2$                               | 1.30E+14 | 0   | 21510 |
| 16. $\text{N}_2\text{H}_4 + \text{M} = \text{NH}_2 + \text{NH}_2 + \text{M}$          | 4.00E+15 | 0   | 41108 |
| 17. $\text{CH}_4 + \text{M} = \text{CH}_3 + \text{H} + \text{M}$                      | 2.00E+17 | 0   | 88430 |
| 18. $\text{CH}_3 + \text{H}_2 = \text{CH}_4 + \text{H}$                               | 6.50E+02 | 3   | 7648  |
| 19. $\text{C}_2\text{H}_6 + \text{M} = \text{CH}_3 + \text{CH}_3 + \text{M}$          | 6.30E+19 | 0   | 82455 |
| 20. $\text{C}_2\text{H}_6 + \text{H} = \text{C}_2\text{H}_5 + \text{H}_2$             | 1.30E+14 | 0   | 9321  |
| 21. $\text{C}_2\text{H}_5 + \text{M} = \text{C}_2\text{H}_4 + \text{H} + \text{M}$    | 1.00E+17 | 0   | 34894 |
| 22. $\text{C}_2\text{H}_6 + \text{CH}_3 = \text{C}_2\text{H}_5 + \text{CH}_4$         | 5.50E-01 | 4   | 8365  |
| 23. $\text{H} + \text{C}_2\text{H}_5 = \text{CH}_3 + \text{CH}_3$                     | 3.00E+13 | 0   | 0     |
| 24. $\text{H} + \text{C}_2\text{H}_5 = \text{C}_2\text{H}_4 + \text{H}_2$             | 1.70E+12 | 0   | 0     |
| 25. $\text{H} + \text{C}_2\text{H}_4 = \text{H}_2 + \text{C}_2\text{H}_3$             | 1.50E+14 | 0   | 10277 |

|     |                        |          |   |       |
|-----|------------------------|----------|---|-------|
| 26. | $C_2H_3+M=C_2H_2+H+M$  | 3.00E+15 | 0 | 32026 |
| 27. | $H+C_2H_3=H_2+C_2H_2$  | 2.00E+13 | 0 | 0     |
| 28. | $CH_3+CH_3=C_2H_4+H_2$ | 1.00E+16 | 0 | 32026 |

Hwang et al. [57] used a similar approach for modeling MMA oxidation at a temperature range from 1260 K to 1600 K, the kinetics model simulation results were consistent with experiment results. The Hwang mechanism contains 141 reactions and 44 species as shown in **Table 4**.

**Table 4.** Hwang et al. [57] chemical kinetics mechanism. Units are  $cm^3/(mol \cdot s)$  for A and cal/mol for E.

Rate constants were expressed as  $k = AT^m \exp(-E/RT)$ .

| <i>Reaction</i> | <i>A</i>                        | <i>m</i> | <i>E</i> |       |
|-----------------|---------------------------------|----------|----------|-------|
| 1.              | $CH_3+NH_2=CH_3NH_2$            | 2.50E+13 | 0        | 0     |
| 2.              | $CH_3+NH_2=CH_2NH_2+H$          | 5.50E+13 | 0        | 11711 |
| 3.              | $CH_3+NH_2=CH_2NH+H_2$          | 6.00E+12 | 0        | 16491 |
| 4.              | $CH_3NH_2=CH_2NH_2+H$           | 1.00E+15 | 0        | 84128 |
| 5.              | $CH_3NH_2+CH_3=CH_2NH_2+CH_4$   | 6.50E+15 | 0        | 27724 |
| 6.              | $CH_3NH_2+NH_2=CH_2NH_2+NH_3$   | 3.30E+15 | 0        | 22227 |
| 7.              | $CH_3NH_2+H=CH_2NH_2+H_2$       | 1.80E+13 | 0        | 5258  |
| 8.              | $CH_3NH_2+H=CH_3+NH_3$          | 3.90E+14 | 0        | 11472 |
| 9.              | $CH_2NH_2=CH_2NH+H$             | 1.00E+13 | 0        | 43020 |
| 10.             | $CH_2NH_2+H=CH_2NH+H_2$         | 1.00E+13 | 0        | 0     |
| 11.             | $CH_2NH+M=CHNH+H+M$             | 1.30E+17 | 0        | 65725 |
| 12.             | $CH_2NH+M=HCN+H_2+M$            | 3.30E+15 | 0        | 38240 |
| 13.             | $CH_2NH+H=CHNH+H_2$             | 5.30E+14 | 0        | 10038 |
| 14.             | $CHNH+M=HCN+H+M$                | 1.60E+15 | 0        | 24856 |
| 15.             | $CHNH+H=HCN+H_2$                | 2.00E+13 | 0        | 0     |
| 16.             | $CH_3NH_2+O_2=CH_2NH_2+HO_2$    | 4.00E+12 | 0        | 42064 |
| 17.             | $CH_3NH_2+O=CH_2NH_2+OH$        | 5.40E+12 | 0        | 1673  |
| 18.             | $CH_3NH_2+OH=CH_2NH_2+H_2O$     | 1.20E+07 | 2        | 1195  |
| 19.             | $CH_3NH_2+HO_2=CH_2NH_2+H_2O_2$ | 1.60E+12 | 0        | 6453  |
| 20.             | $CH_2NH_2+O_2=CH_2NH+HO_2$      | 9.10E+13 | 0        | 9799  |
| 21.             | $CH_2NH_2+O=CH_2NH+OH$          | 5.00E+13 | 0        | 0     |
| 22.             | $CH_2NH_2+OH=CH_2NH+H_2O$       | 5.00E+13 | 0        | 0     |
| 23.             | $CH_2NH+O=CHNH+OH$              | 1.60E+09 | 1.2      | 717   |
| 24.             | $CH_2NH+OH=CHNH+H_2O$           | 6.00E+13 | 0        | 3107  |
| 25.             | $CHNH+O=HCN+OH$                 | 3.00E+13 | 0        | 0     |
| 26.             | $CHNH+OH=HCN+H_2O$              | 3.00E+13 | 0        | 0     |

|     |                   |          |      |       |
|-----|-------------------|----------|------|-------|
| 27. | CH3+CH3=C2H6      | 9.00E+16 | -1.2 | 717   |
| 28. | CH3+CH3=C2H4+H2   | 6.00E+12 | 0    | 16791 |
| 29. | C2H6+CH3=C2H5+CH4 | 5.50E-01 | 4    | 8365  |
| 30. | C2H6+H=C2H5+H2    | 1.30E+14 | 0    | 9321  |
| 31. | C2H5=C2H4+H       | 2.00E+13 | 0    | 39674 |
| 32. | C2H5+H=CH3+CH3    | 3.70E+13 | 0    | 0     |
| 33. | C2H5+H=C2H4+H2    | 1.70E+12 | 0    | 0     |
| 34. | C2H4+M=C2H2+H2+M  | 2.60E+17 | 0    | 79348 |
| 35. | C2H4+M=C2H3+H+M   | 2.60E+17 | 0    | 96556 |
| 36. | C2H4+H=C2H3+H2    | 1.50E+14 | 0    | 10277 |
| 37. | C2H3+H=C2H2+H2    | 2.00E+13 | 0    | 0     |
| 38. | C2H2+H=C2H3       | 5.50E+12 | 0    | 2151  |
| 39. | CH4=CH3+H         | 1.00E+15 | 0    | 99902 |
| 40. | CH4+H=CH3+H2      | 2.20E+04 | 3    | 8843  |
| 41. | CH4+O=CH3+OH      | 1.20E+07 | 2.1  | 7648  |
| 42. | CH4+OH=CH3+H2O    | 1.60E+06 | 2.1  | 2390  |
| 43. | CH3+H=CH2+H2      | 7.20E+14 | 0    | 15057 |
| 44. | CH3+O2=CH3O+O     | 2.20E+14 | 0    | 33699 |
| 45. | CH3+O2=CH2O+OH    | 3.20E+11 | 0    | 9082  |
| 46. | CH3+O=CH2O+H      | 7.00E+13 | 0    | 0     |
| 47. | CH3+OH=CH2+H2O    | 2.00E+13 | 0    | 0     |
| 48. | CH2+H=CH+H2       | 3.00E+13 | 0    | 0     |
| 49. | CH2+O2=CO+OH+H    | 1.30E+13 | 0    | 1434  |
| 50. | CH2+O=CH+OH       | 8.00E+13 | 0    | 0     |
| 51. | CH2+OH=CH+H2O     | 3.00E+13 | 0    | 0     |
| 52. | CH+O2=CO+OH       | 2.00E+13 | 0    | 0     |
| 53. | CH3O+M=CH2O+H+M   | 1.00E+14 | 0    | 25095 |
| 54. | CH2O+M=CHO+H+M    | 5.00E+16 | 0    | 76480 |
| 55. | CH2O+H=CHO+H2     | 2.50E+13 | 0    | 4063  |
| 56. | CH2O+O=CHO+OH     | 3.50E+13 | 0    | 3585  |
| 57. | CH2O+OH=CHO+H2O   | 3.00E+13 | 0    | 1195  |
| 58. | CHO+M=CO+H+M      | 2.50E+14 | 0    | 16730 |
| 59. | CHO+H=CO+H2       | 2.00E+14 | 0    | 0     |
| 60. | CHO+O2=CO+HO2     | 3.00E+12 | 0    | 0     |
| 61. | CHO+O=CO+OH       | 3.00E+13 | 0    | 0     |
| 62. | CHO+OH=CO+H2O     | 5.00E+13 | 0    | 0     |
| 63. | C2H6+O=C2H5+OH    | 3.00E+07 | 2    | 5019  |
| 64. | C2H6+OH=C2H5+H2O  | 6.30E+06 | 2    | 717   |
| 65. | C2H4+O=CH3+CHO    | 1.60E+09 | 1.2  | 717   |
| 66. | C2H4+OH=C2H3+H2O  | 5.00E+13 | 0    | 6692  |
| 67. | C2H3+O2=CH2O+CHO  | 4.00E+12 | 0    | -239  |
| 68. | C2H2+O=CH2+CO     | 4.10E+08 | 1.5  | 1673  |
| 69. | C2H2+O=CHCO+H     | 4.30E+14 | 0    | 12189 |

|      |                        |          |       |       |
|------|------------------------|----------|-------|-------|
| 70.  | $C_2H_2+OH=CH_2CO+H$   | 1.00E+14 | 0     | 11472 |
| 71.  | $CH_2CO+M=CH_2+CO+M$   | 3.60E+15 | 0     | 59272 |
| 72.  | $CHCO+H=CH_2+CO$       | 3.00E+13 | 0     | 0     |
| 73.  | $NH_2+NH_2=N_2H_2+H_2$ | 4.00E+13 | 0     | 11711 |
| 74.  | $NH_2+NH=N_2H_2+H$     | 3.20E+13 | 0     | 956   |
| 75.  | $N_2H_2+M=N_2H+H+M$    | 1.00E+16 | 0     | 49951 |
| 76.  | $N_2H_2+H=N_2H+H_2$    | 5.00E+13 | 0     | 956   |
| 77.  | $NH_3+M=NH_2+H+M$      | 2.50E+16 | 0     | 93688 |
| 78.  | $NH_3+H=NH_2+H_2$      | 1.30E+14 | 0     | 21510 |
| 79.  | $NH_3+O=NH_2+OH$       | 2.20E+13 | 0     | 8843  |
| 80.  | $NH_3+OH=NH_2+H_2O$    | 5.80E+13 | 0     | 8126  |
| 81.  | $NH_2+H=NH+H_2$        | 1.90E+13 | 0     | 0     |
| 82.  | $NH_2+O_2=HNO+OH$      | 1.50E+12 | -0.4  | 36089 |
| 83.  | $NH_2+HO_2=NH_2O+OH$   | 3.00E+13 | 0     | 21988 |
| 84.  | $NH_2+NO=N_2H+OH$      | 8.80E+15 | -1.25 | 0     |
| 85.  | $NH_2+NO=N_2+H_2O$     | 6.30E+19 | -2.5  | 1912  |
| 86.  | $NH_2+O=HNO+H$         | 8.90E+14 | -0.5  | 239   |
| 87.  | $NH_2+O=NH+OH$         | 6.90E+11 | 0.4   | -239  |
| 88.  | $NH_2+OH=NH+H_2O$      | 5.00E+11 | 0.5   | 1912  |
| 89.  | $NH+H=N+H_2$           | 1.00E+14 | 0     | 0     |
| 90.  | $NH+O_2=NO+OH$         | 1.40E+11 | 0     | 1912  |
| 91.  | $NH+O_2=HNO+O$         | 1.00E+13 | 0     | 11950 |
| 92.  | $NH+NO=N_2O+H$         | 1.70E+14 | -0.5  | 0     |
| 93.  | $NH+O=NO+H$            | 6.30E+11 | 0.5   | 0     |
| 94.  | $NH+OH=HNO+H$          | 1.50E+12 | 0.5   | 1912  |
| 95.  | $NH+OH=N+H_2O$         | 5.00E+11 | 0.5   | 1912  |
| 96.  | $NH_2O+M=HNO+H+M$      | 3.60E+13 | 0     | 25095 |
| 97.  | $N+O_2=NO+O$           | 6.00E+09 | 1     | 6214  |
| 98.  | $N_2+O=N+NO$           | 1.80E+14 | 0     | 76241 |
| 99.  | $NO+H=N+OH$            | 1.70E+14 | 0     | 48756 |
| 100. | $HNO+M=H+NO+M$         | 1.90E+16 | 0     | 48756 |
| 101. | $HNO+H=NO+H_2$         | 1.30E+13 | 0     | 4063  |
| 102. | $HNO+OH=NO+H_2O$       | 3.60E+13 | 0     | 0     |
| 103. | $N_2H+M=N_2+H+M$       | 2.00E+14 | 0     | 5975  |
| 104. | $N_2H+NO=N_2+HNO$      | 2.50E+12 | 0     | 0     |
| 105. | $N_2O+M=N_2+O+M$       | 6.90E+23 | -2.5  | 65008 |
| 106. | $N_2O+H=N_2+OH$        | 7.60E+13 | 0     | 15057 |
| 107. | $N_2O+O=NO+NO$         | 1.00E+14 | 0     | 27963 |
| 108. | $HCN+O=CN+OH$          | 5.00E+13 | 0     | 21988 |
| 109. | $HCN+O=NCO+H$          | 1.70E+08 | 1.5   | 7409  |
| 110. | $HCN+O=NH+CO$          | 2.20E+13 | 0     | 15296 |
| 111. | $HCN+OH=CN+H_2O$       | 4.40E+12 | 0     | 9082  |
| 112. | $CN+H_2=HCN+H$         | 2.50E+02 | 3.62  | 912   |

|      |                 |          |      |       |
|------|-----------------|----------|------|-------|
| 113. | CN+O2=NCO+O     | 5.60E+12 | 0    | 0     |
| 114. | CN+O=CO+N       | 2.00E+13 | 0    | 478   |
| 115. | CN+OH=NCO+H     | 5.60E+13 | 0    | 0     |
| 116. | NCO+M=CO+N+M    | 6.30E+16 | -0.5 | 47800 |
| 117. | NCO+H2=HNCO+H   | 3.00E+13 | 0    | 5258  |
| 118. | NCO+H=NH+CO     | 4.00E+13 | 0    | 0     |
| 119. | NCO+NO=N2O+CO   | 1.00E+13 | 0    | -478  |
| 120. | NCO+O=NO+CO     | 5.80E+13 | 0    | 0     |
| 121. | HNCO+M=NH+CO+M  | 5.00E+13 | 0    | 70027 |
| 122. | HNCO+H=NH2+CO   | 2.00E+13 | 0    | 3107  |
| 123. | HNCO+O2=NCO+HO2 | 1.00E+13 | 0    | 70027 |
| 124. | H2+M=H+H+M      | 2.20E+14 | 0    | 96078 |
| 125. | H+O2=OH+O       | 2.20E+14 | 0    | 16730 |
| 126. | O+H2=OH+H       | 1.50E+07 | 2    | 7648  |
| 127. | OH+H2=H2O+H     | 1.00E+08 | 1.6  | 3346  |
| 128. | OH+OH=H2O+O     | 1.50E+09 | 1.14 | 0     |
| 129. | H+O2+M=HO2+M    | 2.50E+15 | 0    | 0     |
| 130. | H+OH+M=H2O+M    | 7.50E+23 | -2.6 | 0     |
| 131. | HO2+H=OH+OH     | 2.50E+14 | 0    | 1912  |
| 132. | HO2+H=H2+O2     | 2.50E+13 | 0    | 717   |
| 133. | HO2+OH=H2O+O2   | 2.00E+13 | 0    | 0     |
| 134. | HO2+O=OH+O2     | 2.00E+13 | 0    | 0     |
| 135. | HO2+HO2=H2O2+O2 | 2.00E+12 | 0    | 0     |
| 136. | H2O2+M=OH+OH+M  | 1.20E+17 | 0    | 45410 |
| 137. | CO+OH=CO2+H     | 4.40E+06 | 1.5  | -717  |
| 138. | CH3+NO=HCN+H2O  | 4.30E+12 | 0    | 20315 |
| 139. | CH2+NO=HCN+OH   | 1.40E+12 | 0    | -1195 |
| 140. | CH+NO=HCN+O     | 1.20E+14 | 0    | 0     |
| 141. | CH+N2=HCN+N     | 2.10E+12 | 0    | 16730 |

The previously reported chemical kinetics mechanisms were proposed for reaction temperatures in excess of 1225 K. Additionally, the mechanism by Higashihara et al. [57] contains no reactions that include the species NO and NO<sub>2</sub>.

Other available mechanisms for MMA, such as by Coda et al. [58], and Dean and Bozzelli [59], were also proposed for high temperature MMA oxidation and might not be

able to predict the chemistry of an MMA-based SNCR NO<sub>x</sub> process with a good degree of accuracy.

Kantak et al. [60] conducted studies on MMA oxidation modeling at temperatures from 600 K to 1400 K. Chemical reaction predictions from the Kantak et al.'s [60] mechanism, which has 350 reactions and 65 species, showed good agreement with experimental data from Hjuler et al. [61] in the temperature range from 600 K to 1400 K, thereby becoming a good candidate to be used for MMA-based SNCR NO<sub>x</sub> reduction simulations.

### **3.3 Plug Flow Reactor Modeling**

A plug flow reactor (PFR) modeling approach was used in this study to investigate the progress of the chemistry of MMA for SNCR applications. Plug flow reactor modeling is a chemical numerical model that describes an ideal plug flow with the following assumption:

- (1) No temperature or species concentration gradient in the radial direction, that is, on each cross-section plane in the flow direction, the temperature is constant and every chemical species on the cross-section is evenly distributed;
- (2) No back-mixing, that is, the species are perfectly mixed in the radial direction but not in the axial direction.

A schematic of the PFR concept is shown **Figure 12**.

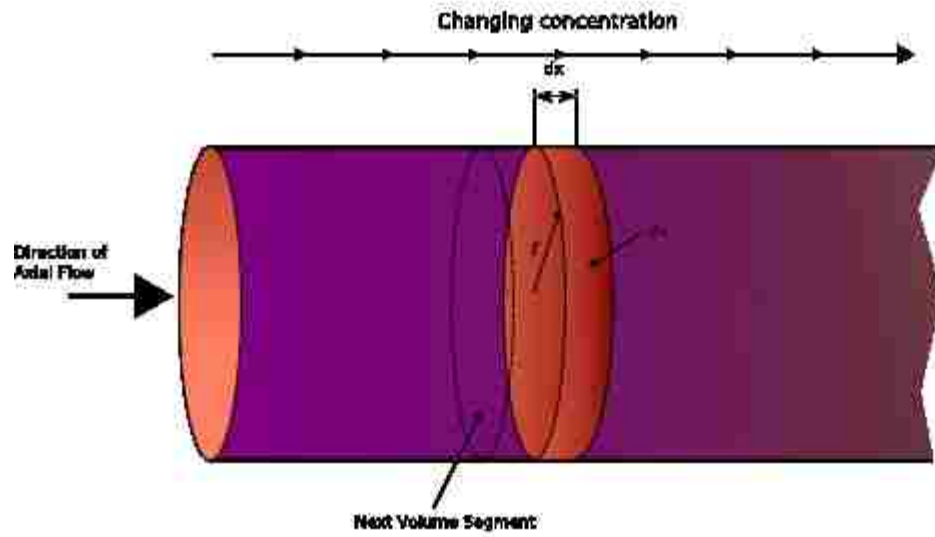


Figure 12. Schematic diagram of a plug flow reactor.

The species concentration part of the PFR model is governed by ordinary differential equations and the problem can be defined by the mass balance equation:

$$[\text{accumulation}] = [\text{in}] - [\text{out}] + [\text{generation}] - [\text{consumption}] \quad \text{Eq. 1}$$

Assuming the system is at steady state, then accumulation is 0, hence Eq. 1 can be re-written as:

$$F(x) - F(x + dx) + A \cdot v \cdot r \cdot dx = 0 \quad \text{Eq. 2}$$

Where:  $x$  is the axial position in the reactor

$dx$  is the differential thickness of the fluid plug

$F(x)$  is the molar flow rate of species

$A$  is the cross sectional area

$v$  is the stoichiometric coefficient

$r$  is the volumetric reaction rate

Considering a flow linear velocity of  $u$ , concentration of species  $C$  and the assumption that  $dx \rightarrow 0$ , the above equation can be re-written as:

$$u \frac{dC}{dx} = vr \quad \text{Eq. 3}$$

or,

$$\frac{dC}{dt} = vr \quad \text{Eq. 4}$$

Where :  $t$  is time

$r$  can be calculated by the equation:

$$r = k(T)[\text{reactant A}]^n[\text{reactant B}]^m \quad \text{Eq. 5}$$

Where:  $m$  and  $n$  are the partial orders of the reactions and depend on the reaction mechanism.

$k(T)$  is defined by the modified Arrhenius expression:

$$k(T) = AT^m e^{(-E/RT)} \quad \text{Eq. 6}$$

Where:  $A$  is the pre-exponential constant

$m$  is the temperature exponent

$E$  is the activation energy

$R$  is the universal gas constant

$T$  is the temperature

Solving the Equations 1 to 6 with initial conditions, which are the PFR inlet conditions; and the parameters from the kinetics mechanism list, the results of the simulation can be obtained.

Despite the limitation that the PFR model is one-dimensional, thereby it does not handle spatial variations in temperature and velocity at a given multiple-dimensional space,

it can still provide reliable results for the study of the potential of the NO<sub>x</sub> reduction performance of different alternative reagents for the SNCR process.

### **3.4 Model Validation**

The model validations were performed using the CHEMKIN package and the SENKIN subroutine.

The CHEMKIN package is an interpreter program that reads the symbolic description of a given chemical reaction mechanism and the thermodynamic database which includes the thermodynamic properties of the relevant species. The output of the program is a data file which links to the CHEMKIN subroutine library and it can return the information on species and reactions and their production rates. The linking file can be considered as part of the input to the SENKIN code.

The SENKIN code is a plug flow model subroutine which can be coded as a program that reads in several parameters such as initial temperature, temperature slope (along the plug flow reactor), reaction pressure, residence time, input species and their concentrations and it conducts calculations based on the mentioned linking file to simulate the rate of progress of chemical mechanism under certain conditions. The CHEMKIN and SENKIN model structure is shown in **Figure 13**.

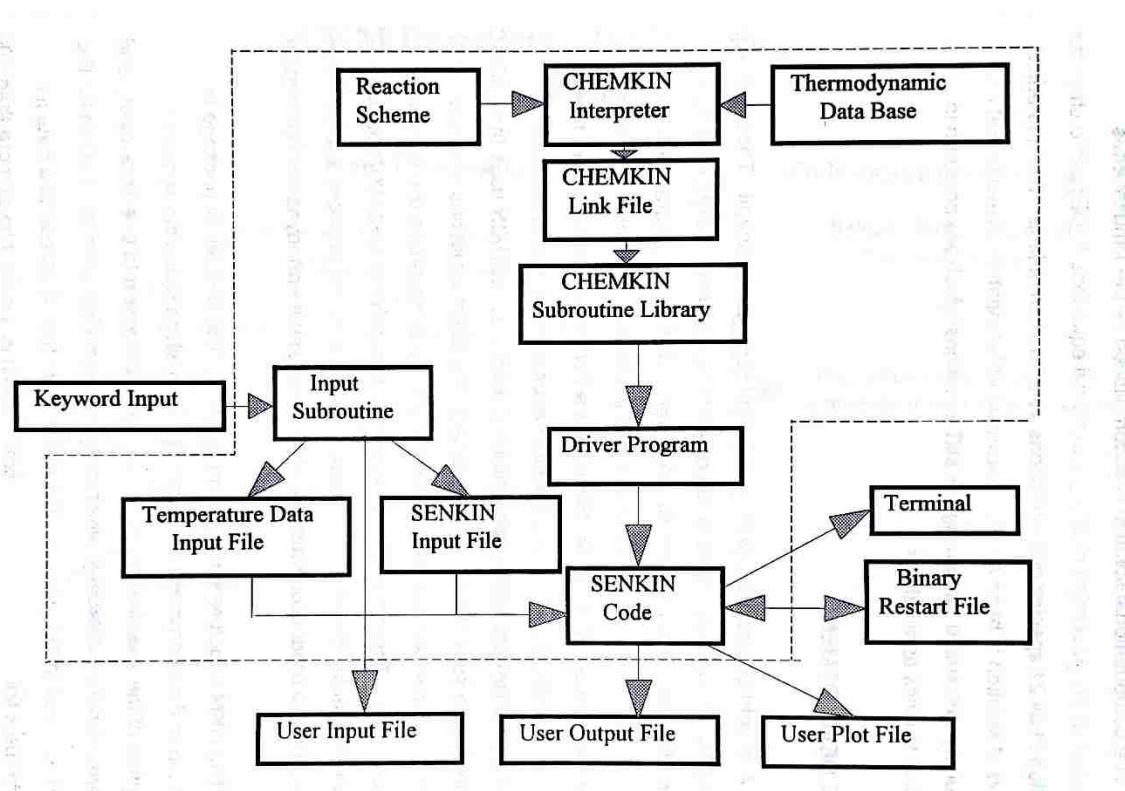


**Figure 13.** Chemical kinetics modeling by implementing CHEMKIN and SENKIN [63].

PFR modeling with CHEMKIN and SENKIN was executed with the kinetics mechanisms listed in Section 3.2 to validate their chemical kinetics scheme capabilities for simulating the MMA-based SNCR NO<sub>x</sub> reduction process. A first validation was done by comparing the simulation data (Simul. Data) from the MMA kinetics mechanisms by Hwang et al. [57], Coda et al. [58] and Kantak et al. [60] with experimental data (Exp. Data) by Hjuler et al. [61]. The results of the simulations are presented below (**Figures 14 to 16**).

As previously discussed, **Figure 14** clearly illustrates that the mechanism by Hwang et al. [57] is not able to follow the MMA – NO/NO<sub>2</sub> experimental results, with a very poor agreement with the experimental data. Similarly, results obtained from simulations using the chemical kinetics scheme by Coda et al. [58] (**Figure 15**) are also in poor agreement.

Both mechanisms by Hwang et al. [57] and Coda et al. [58] are not capable of predicting formation of NO<sub>2</sub>. Therefore, the mechanisms that were developed for a high temperature environment are not a proper choice for low-temperature SNCR NO<sub>x</sub> reduction process simulation.

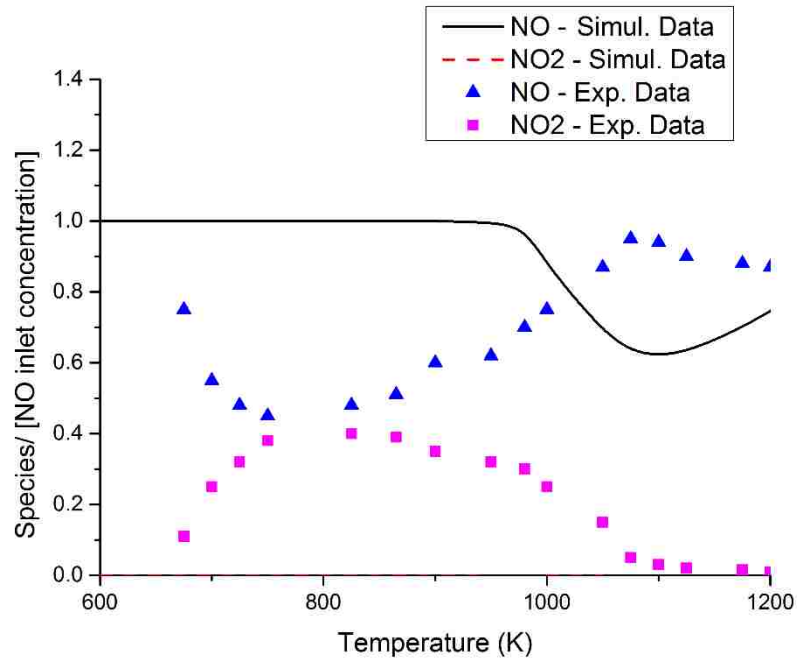


**Figure 14.** Comparison between experimental data by Hjuler et al. [61] and the simulation predictions by using the mechanism by Hwang et al. [57] for species NO and NO<sub>2</sub>. Inlet conditions: 1.0 atm; 600 K – 1200 K; residence time = 0.2 s; (in mole %) [CH<sub>3</sub>NH<sub>2</sub>] = 0.026, [NO] = 0.0471, [O<sub>2</sub>] = 4.0, [H<sub>2</sub>O] = 0.1, balance nitrogen.

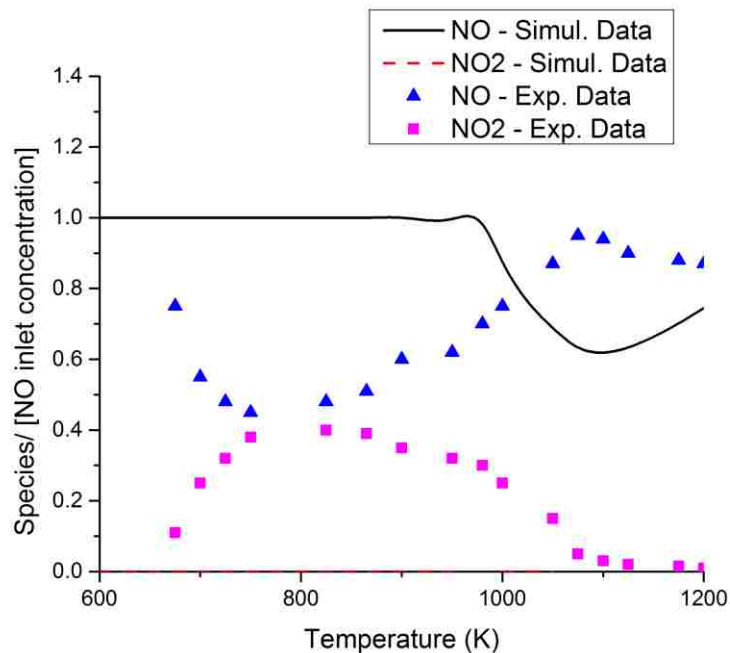


**Figure 15.** Comparison between experimental data by Hjuler et al. [61] and the simulation predictions by using the mechanism by Coda et al. [58] for species NO and NO<sub>2</sub>. Inlet conditions: 1.0 atm; 600 K – 1200 K; residence time = 0.2 s; (in mole %) [CH<sub>3</sub>NH<sub>2</sub>] = 0.026, [NO] = 0.0471, [O<sub>2</sub>] = 4.0, [H<sub>2</sub>O] = 0.1, balance nitrogen.

In **Figure 16**, the simulation results from the mechanism by Kantak et al. [60] are relatively consistent with the experimental data by Hjuler et al. [61] especially at the points around the peak NO reduction. However, at temperatures below 800 K, the differences between the simulation data and the experimental data become significant. The mechanism by Kantak et al. [60] also provides NO<sub>2</sub> predictions that are in line with the experimental data.

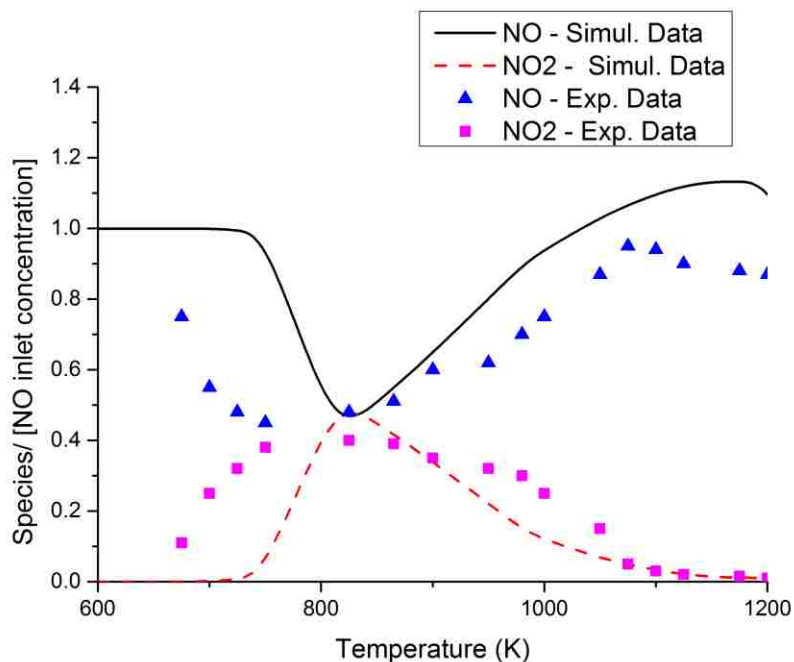


**Figure 16.** Comparison between experimental data by Hjuler et al. [61] and the simulation predictions by using mechanism by Kantak et al. [60] for species NO and NO<sub>2</sub>. Inlet conditions: 1.0 atm; 600 K – 1200 K; residence time = 0.2 s; (in mole %) [CH<sub>3</sub>NH<sub>2</sub>] = 0.026, [NO] = 0.0471, [O<sub>2</sub>] = 4.0, [H<sub>2</sub>O] = 0.1, balance nitrogen.

**Figure 17** presents another validation for the mechanism by Kantak et al. [60] with reference from experimental data by Milewska [64]. These data were produced by the Institute of Power Engineering in Poland to evaluate the NO reduction capability of MMA in the laboratory data. The comparison shows not a perfect agreement with the data; however, for some conditions, the model provides a good level of prediction accuracy.

It can be seen in **Figure 17** that there are three groups of data (data that falls on the 45 degree line, and two other groups of data above and below this line). The predicted trend for all three groups are correct, indicating that there may have been a drift in the laboratory measurements reported by the Institute of Power Engineering in Poland.

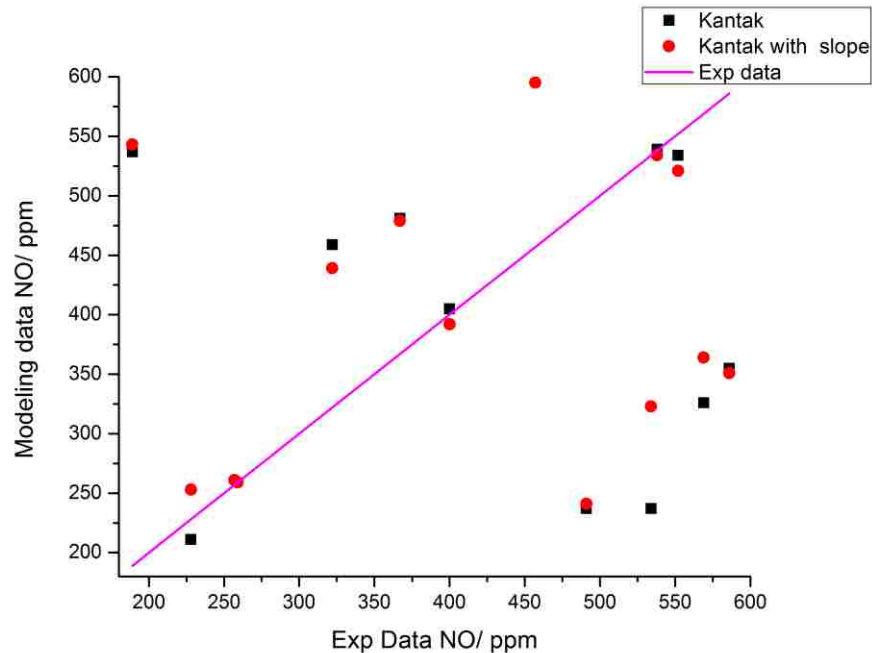


**Figure 17.** Comparison between experimental data by Milewska [64] and the simulation predictions by using mechanism by Kantak et al. [60] for outlet NO concentration. The inlet condition is varied and corresponding to different cases. The temperature slope for the simulation that is with slope is 100 K/s.

In summary, the mechanism by Kantak et al. [60] is arguably the most promising MMA-NO reaction mechanism for modeling the MMA-based SNCR NO<sub>x</sub> reduction process, despite its limitation in accurately matching experimental data at lower temperatures. A sensitive analysis was performed and reported in Section 3.5. This was done to obtain a better understanding of the features related to the MMA NO<sub>x</sub> reduction process.

### 3.5 Sensitive Analysis

Sensitive analysis helps understand the impact of different parameters on the output of the simulation under specified inlet conditions. This section discusses the influence of the following parameters: normalized stoichiometric ratio (NSR, defined as the actual mole

ratio of the reagent, MMA in this case, to NO), initial CO and NO concentration, residence time and temperature. In **Table 5**, simulation baseline conditions are underlined. Sensitivity results are provided in terms of outlet NO, NO<sub>2</sub>, NH<sub>3</sub> and HCN. The range of the parameters for the simulations of the sensitivity analysis are listed in **Table 5**.

**Table 5.** Inlet conditions for sensitive analysis. \*The underline values are the baseline conditions.

|                     |                       |
|---------------------|-----------------------|
| Temp /K             | 600-1400              |
| Residence time /s   | 0.1, <u>0.3</u> , 0.5 |
| NO /ppm             | 50, <u>500</u> , 800  |
| O <sub>2</sub> /%   | <u>4</u>              |
| CO <sub>2</sub> /%  | <u>10</u>             |
| CO /ppm             | <u>0</u> , 10, 100    |
| NSR                 | 0.25, <u>0.5</u> , 1  |
| H <sub>2</sub> O /% | <u>5</u>              |
| N <sub>2</sub> /%   | Balance               |

### 3.5.1 NSR Simulations

**Figure 18** shows an optimal temperature window for the reaction of NO by MMA. This window is from approximately 750 K to 1000 K. These temperature levels are relatively lower than those of the NH<sub>3</sub> and urea processes. NO reductions up to 90% can be theoretically achieved with a NSR of 1.0 and at about 800 K. NO<sub>2</sub> production as high as 380 ppm can be achieved at that 1.0 NSR. HCN emissions as high as 90 ppm can result from injection of MMA at the NSR of 1.0.

Simulations with different NSRs show that NSR has a great impact on NO, NO<sub>2</sub> and HCN reduction/production, while the influence is relatively small on NH<sub>3</sub> formation (see **Figures 18 to 20**). Note that predicted HCN emissions is of a concern, while NH<sub>3</sub> slip from the process is rather negligible, at less than 3 ppm (see **Figures 19 and 20**).

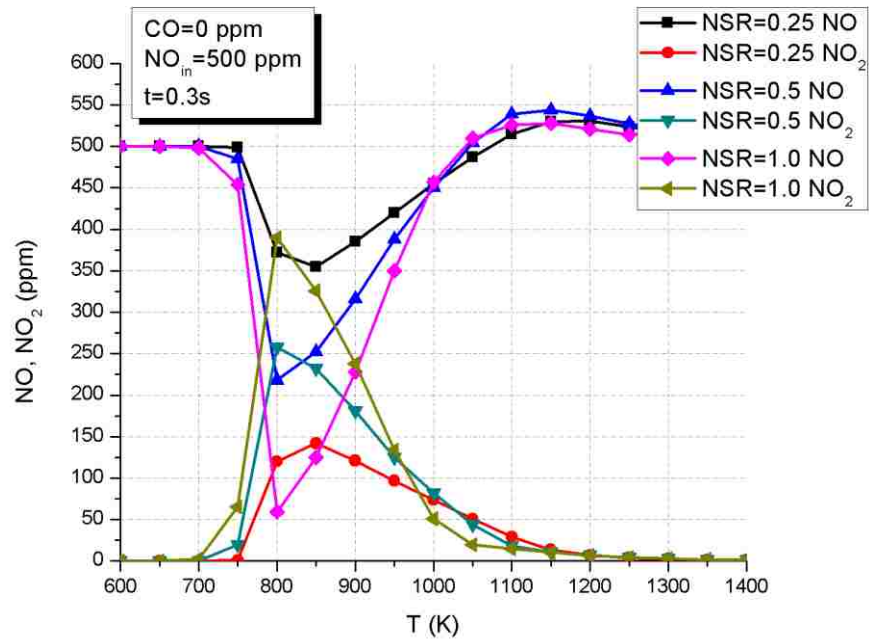


Figure 18. Predicted outlet NO and NO<sub>2</sub> concentrations vs. temperature under various NSRs.

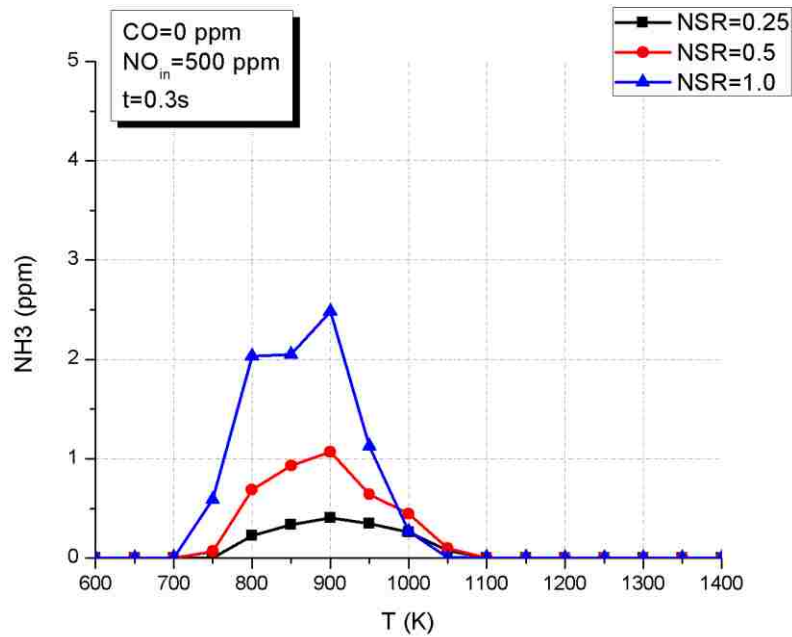
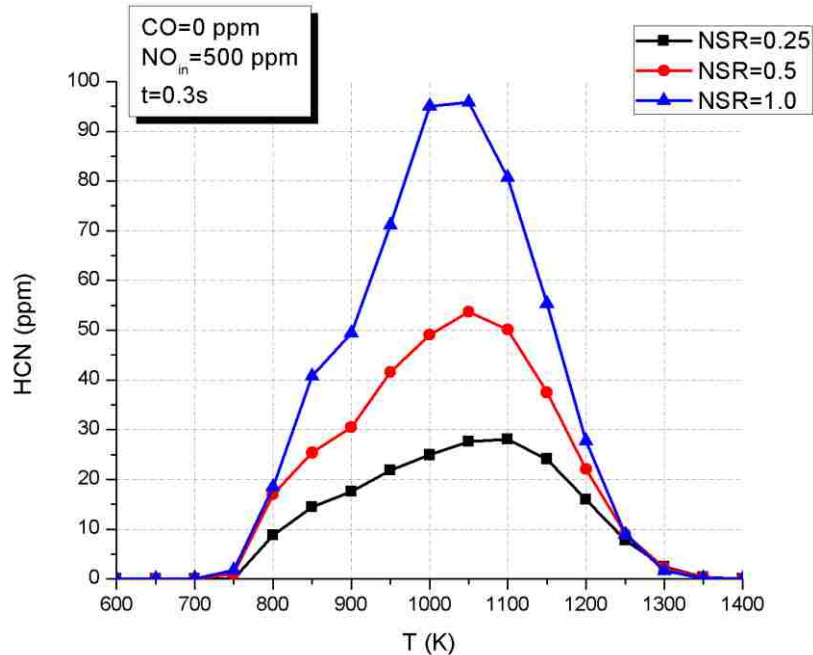


Figure 19. Predicted outlet NH<sub>3</sub> concentrations vs. temperature under various NSRs.



**Figure 20.** Predicted outlet HCN concentrations vs. temperature under various NSRs.

### 3.5.2 Initial CO Concentration Simulations

**Figures 21 to 23** show simulations including different initial CO concentrations and indicate that the inlet CO level has a negligible impact particularly at low temperatures on NH<sub>3</sub> and HCN emissions, but a greater impact on NO and NO<sub>2</sub> reduction/production. At high CO levels, the temperature window for MMA to react with NO seems to significantly widen and the reactions starts to take place below 700 K. NO<sub>2</sub> production also increases at high CO levels. These results are in line with the report by Lodder and Lefers [26] that CO addition can accelerate the reduction process of NO<sub>x</sub> by NH<sub>3</sub>, considerably shifting downward the optimal reaction temperature of MMA.

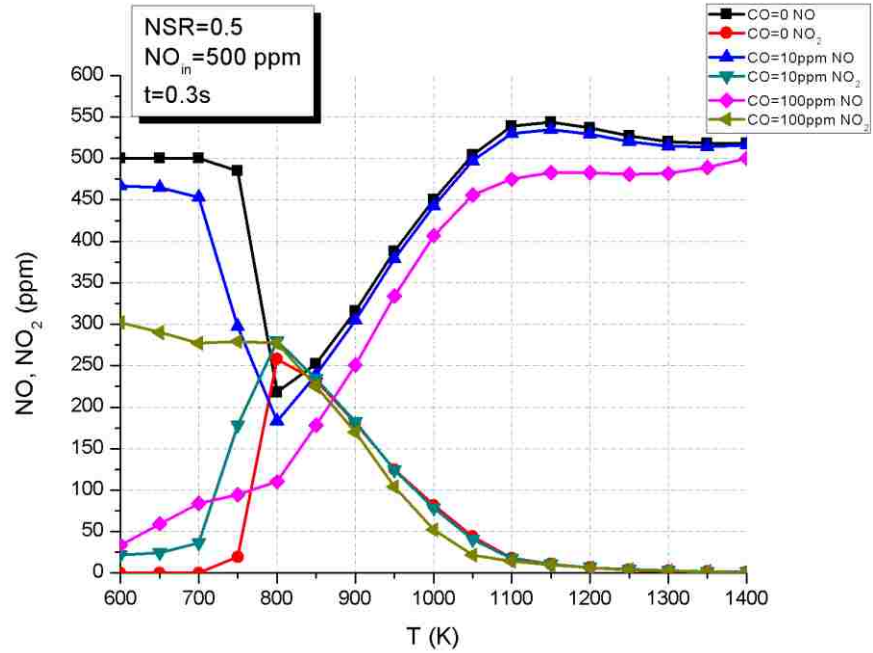


Figure 21. Predicted outlet NO and NO<sub>2</sub> concentrations vs. temperature under various initial CO concentrations.

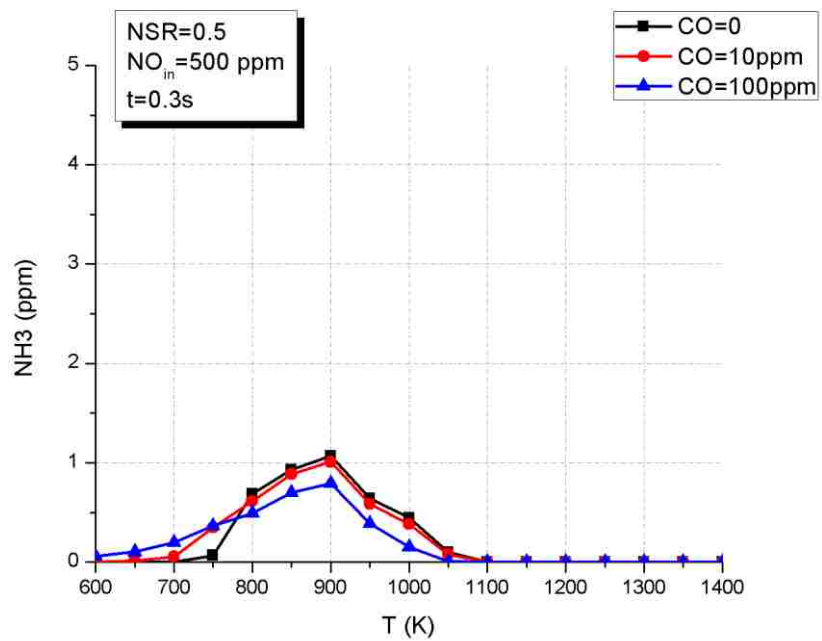
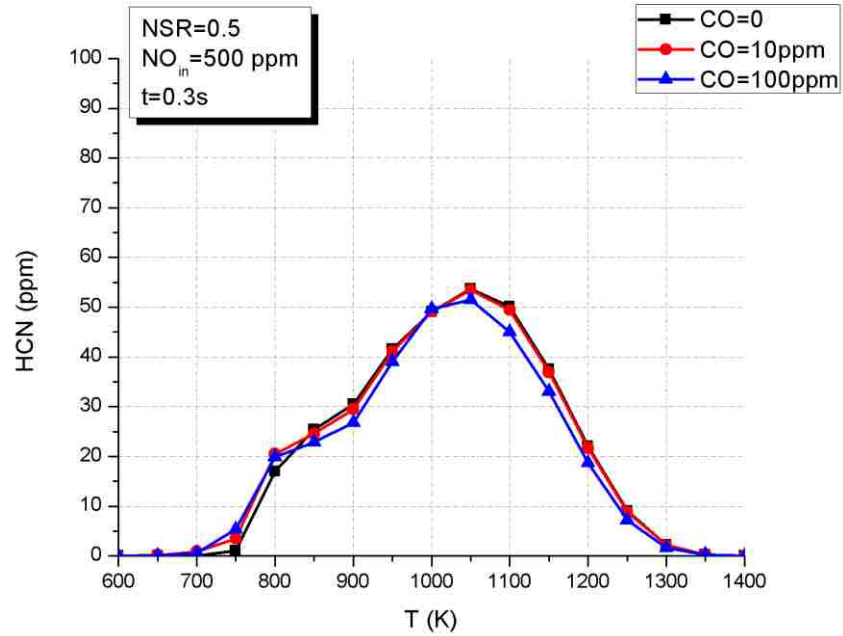


Figure 22. Predicted outlet NH<sub>3</sub> concentrations vs. temperature under various initial CO concentrations.



**Figure 23.** Predicted outlet HCN concentrations vs. temperature under various initial CO concentrations.

### 3.5.3 Initial NO Concentration Simulations

The results at different inlet NO levels (**Figures 24 to 26**) are consistent with results previously obtained in this study. The percentage of NO reduction for the different initial levels are 50%, 55% and 52.5%, for NO = 50 ppm, 500 ppm and 800 ppm, respectively. The HCN and NH<sub>3</sub> slip result at different initial NO levels are consistent with the MMA increased injection level to maintain a NSR of 0.5 for the simulations.

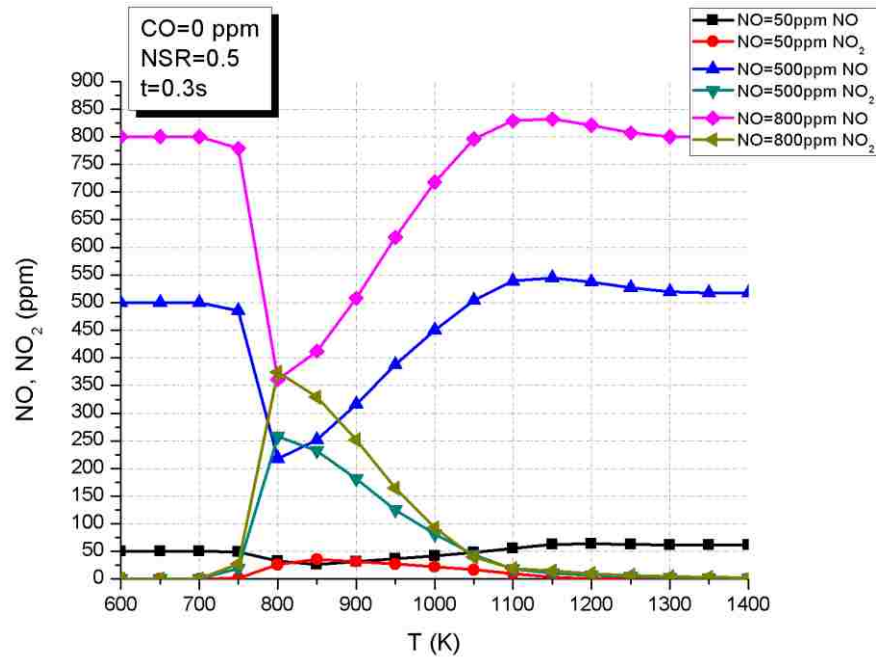


Figure 24. Predicted outlet NO and NO<sub>2</sub> concentrations vs. temperature under various initial NO concentrations.

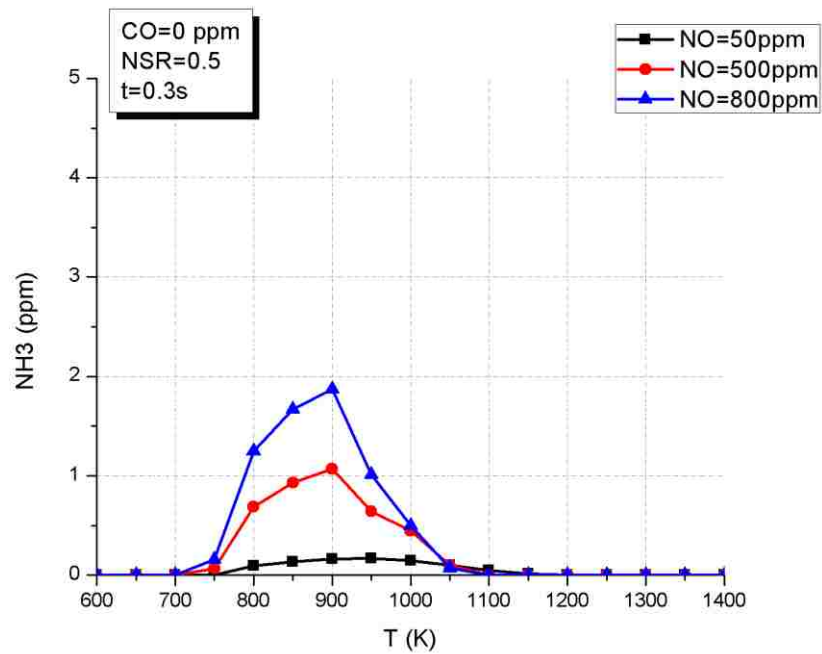
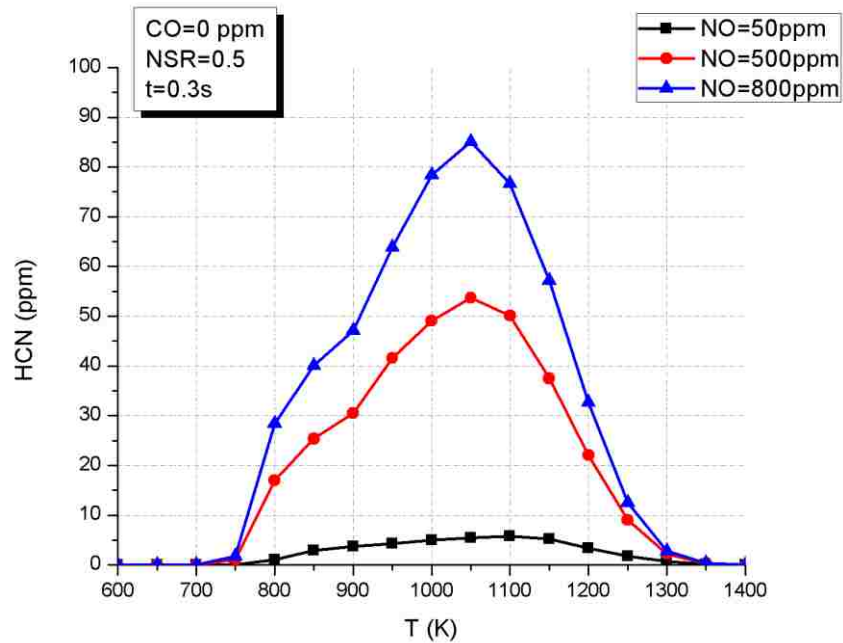


Figure 25. Predicted outlet NH<sub>3</sub> concentrations vs. temperature under various initial NO concentrations.



**Figure 26.** Predicted outlet  $\text{NH}_3$  concentrations vs. temperature under various initial NO concentrations.

### 3.5.4 Residence Time Simulations

The residence time simulations suggest that the residence time tends to shift the temperature window to the left for all the parameters of interest (see **Figures 27 to 29**). This is because the  $\text{NO}_x$  reduction process by MMA requires longer than 0.3 sec to complete the reaction.

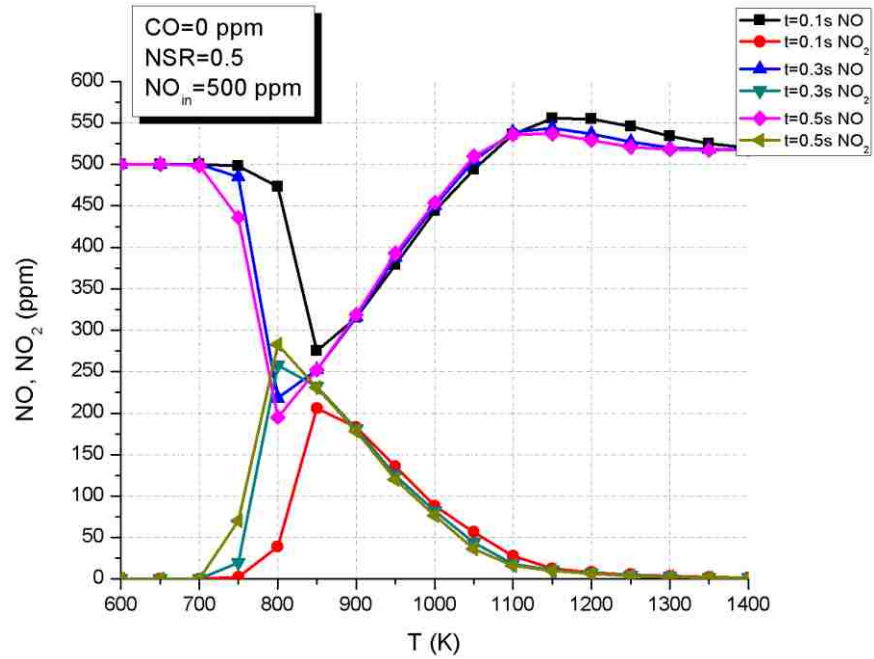


Figure 27. Predicted outlet NO and NO<sub>2</sub> concentrations vs. temperature under various residence times.

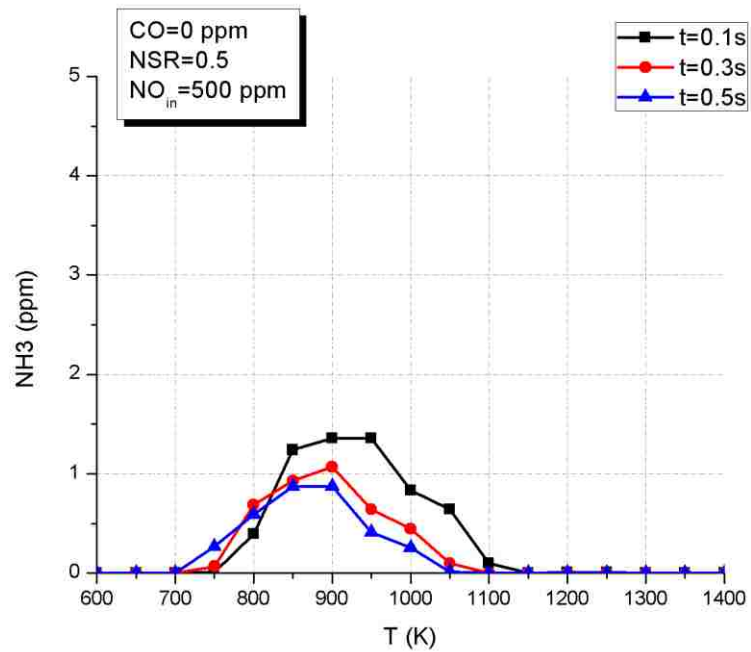
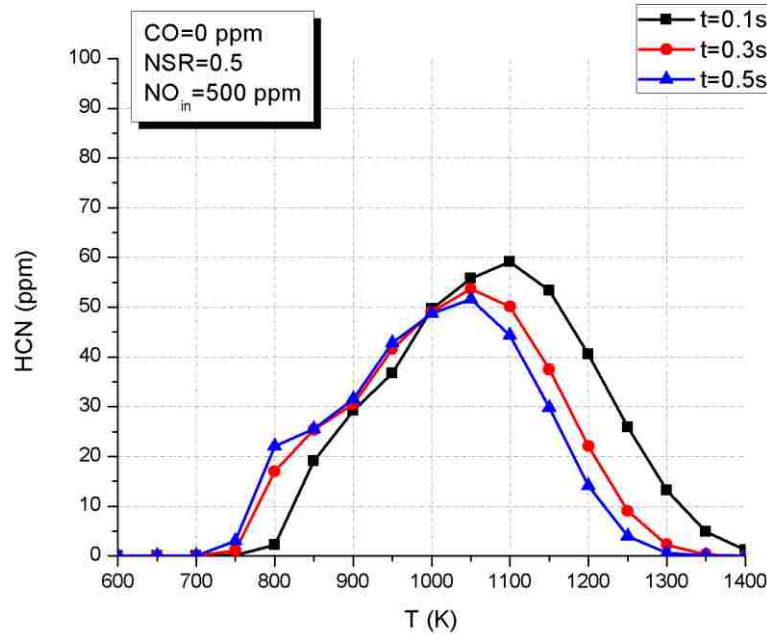


Figure 28. Predicted outlet NH<sub>3</sub> concentrations vs. temperature under various residence times.



**Figure 29.** Predicted outlet HCN concentrations vs. temperature under various residence times.

According to the sensitivity simulation results, NSR and initial NO concentration are identified to be the most critical parameters that significantly affect the outcome of the kinetics of MMA under SNCR conditions. The results are also in line with the results reported in the literature, that CO addition to the NO reduction process can shift the optimal reaction temperature of the reducing process.

### 3.6 Monomethylamine Kinetics Mechanism Reduction

The goal of chemical kinetics mechanism reduction is to introduce a reduced mechanism model which has relatively less species and reactions than the detailed one does, helping in that it can be easily fitted into full computational fluid mechanics (CFD) simulations.

Typical approaches for the mechanism reduction include a combination of rate of production and rate of reaction analysis. In this study, a rate of production analysis was

used to evaluate the contribution to the molar rate of production of each species in the MMA chemical kinetics mechanism from each reaction. A temperature range from 200 K to 900 K was used in the analysis. Reactions that showed negligible effect to the evaluation of major chemical species, MMA ( $\text{CH}_3\text{NH}_2$ ), NO, NO<sub>2</sub>, N<sub>2</sub>O, CO, NH<sub>3</sub> and HCN, were temporally eliminated. Then the modified mechanism was tested with SENKIN code under the baseline conditions presented in the caption of **Table 6**, and the simulation results were compared with the results from the original detailed mechanism by Kantak et al. [60], under the same initial conditions. Once the comparison results showed acceptable differences (less than 10% of the concentrations) for most cases, the temporally eliminated reactions were considered not critical to the entire mechanism and removed permanently. Following the above procedure, the comparison of simulation results between the full mechanism by Kantak et al. [60] and the reduce mechanism is listed in **Table 6**. According to the data in **Table 6**, the reduced mechanism shows decent agreement with the original mechanism by Kantak et al. [60] despite the fact that relative errors at some temperatures for several species exceed 10%. However, since that the actual value of the concentration of the species whose relative error is larger than 10% is sufficiently small, the mentioned data pair can be still considered as in good agreement. For example at 775 K,  $[\text{NO}]_{\text{ORG}} = 2.1$  ppm and  $[\text{NO}]_{\text{RED}} = 1.59$  ppm and the difference between the two result is just 0.51 ppm.

**Table 6.** Simulation result comparison between reduced mechanism and original mechanism by Kantak et al. [60]. Inlet condition: 1.0 atm; 700 K – 900 K; residence time = 1.0s; (in mole %) [CH<sub>3</sub>NH<sub>2</sub>] = 0.01, [NO] = 0.01, [O<sub>2</sub>] = 11.75, [H<sub>2</sub>O] = 9.95, [CO<sub>2</sub>] = 4.12, balance nitrogen. ORG – original Kantak et al.’s, RED – reduced Kantak et al.’s, Δ% - the relative error =  $\frac{[ORG\ species] - [RED\ species]}{[ORG\ species]} \times 100\%$ .

|         | NO                              |         |        | NO <sub>2</sub>  |         |        |
|---------|---------------------------------|---------|--------|------------------|---------|--------|
| TEMP/ K | ORG/ppm                         | RED/ppm | Δ%     | ORG/ppm          | RED/ppm | Δ%     |
| 700     | 82.8                            | 82.7    | 0.10%  | 24               | 24.1    | 0.40%  |
| 725     | 42.7                            | 42.9    | 0.50%  | 90.8             | 90.7    | 0.10%  |
| 750     | 6.48                            | 6.01    | 7.30%  | 156              | 157     | 0.60%  |
| 775     | 2.1                             | 1.59    | 24.30% | 166              | 166     | 0.00%  |
| 800     | 7.1                             | 6.3     | 11.30% | 162              | 162     | 0.00%  |
| 825     | 14.7                            | 13.8    | 6.10%  | 154              | 155     | 0.60%  |
| 850     | 22.9                            | 21.8    | 4.80%  | 147              | 148     | 0.70%  |
| 875     | 30.9                            | 29.6    | 4.20%  | 139              | 140     | 0.70%  |
| 900     | 38.7                            | 37      | 4.40%  | 131              | 132     | 0.80%  |
|         | NH <sub>3</sub>                 |         |        | N <sub>2</sub> O |         |        |
| TEMP/ K | ORG/ppm                         | RED/ppm | Δ%     | ORG/ppm          | RED/ppm | Δ%     |
| 700     | 0.00565                         | 0.00514 | 9.00%  | 1.29             | 1.14    | 11.60% |
| 725     | 0.0473                          | 0.0479  | 1.30%  | 6.41             | 6.4     | 0.20%  |
| 750     | 0.0891                          | 0.09    | 1.00%  | 9.6              | 9.61    | 0.10%  |
| 775     | 0.131                           | 0.134   | 2.30%  | 9.39             | 9.4     | 0.10%  |
| 800     | 0.184                           | 0.191   | 3.80%  | 8.67             | 8.69    | 0.20%  |
| 825     | 0.245                           | 0.265   | 8.20%  | 7.87             | 7.91    | 0.50%  |
| 850     | 0.307                           | 0.349   | 13.70% | 7.08             | 7.16    | 1.10%  |
| 875     | 0.355                           | 0.429   | 20.80% | 6.37             | 6.48    | 1.70%  |
| 900     | 0.387                           | 0.485   | 25.30% | 5.73             | 5.89    | 2.80%  |
|         | CH <sub>3</sub> NH <sub>2</sub> |         |        | HCN              |         |        |
| TEMP/ K | ORG/ppm                         | RED/ppm | Δ%     | ORG/ppm          | RED/ppm | Δ%     |
| 700     | 71.3                            | 71.2    | 0.10%  | 1.13             | 1.14    | 0.90%  |
| 725     | 24.8                            | 24.9    | 0.40%  | 3.84             | 3.89    | 1.30%  |
| 750     | 3.07                            | 3.04    | 1.00%  | 7.04             | 7.2     | 2.30%  |
| 775     | 0.448                           | 0.477   | 6.50%  | 8.91             | 9.26    | 3.90%  |
| 800     | 0.117                           | 0.136   | 16.20% | 9.94             | 10.3    | 3.60%  |
| 825     | 0.0425                          | 0.0551  | 29.60% | 11.1             | 11.4    | 2.70%  |
| 850     | 0.0147                          | 0.0228  | 55.10% | 12.3             | 12.5    | 1.60%  |
| 875     | 0.00368                         | 0.00723 | 96.50% | 13.6             | 13.7    | 0.70%  |
| 900     | 0.000704                        | 0.00128 | 81.80% | 14.7             | 14.8    | 0.70%  |
|         | CO                              |         |        |                  |         |        |
| TEMP/ K | ORG/ppm                         | RED/ppm | Δ%     |                  |         |        |
| 700     | 1.21                            | 1.21    | 0.00%  |                  |         |        |
| 725     | 15.7                            | 15.5    | 1.30%  |                  |         |        |
| 750     | 47.3                            | 47.4    | 0.20%  |                  |         |        |
| 775     | 58                              | 58      | 0.00%  |                  |         |        |
| 800     | 60.3                            | 60.4    | 0.20%  |                  |         |        |
| 825     | 60.9                            | 61.2    | 0.50%  |                  |         |        |
| 850     | 60.9                            | 61.4    | 0.80%  |                  |         |        |
| 875     | 59.9                            | 60.8    | 1.50%  |                  |         |        |
| 900     | 58.2                            | 59      | 1.40%  |                  |         |        |

Using the mentioned approach, a reduced kinetic mechanism that contains 36 species and 67 reactions (derived from 65 species and 350 reactions by Kantak et al. [60]) is proposed. The reduced mechanism (RM) is shown in **Table 7**.

**Table 7.** Reduced mechanism. Units are  $\text{cm}^3/(\text{mol}\cdot\text{s})$  for  $A$  and  $\text{cal/mol}$  for  $E$ . Rate constants were expressed as  $k = AT^m \exp(-E/RT)$ .

| Reactions  | $A$      | $m$  | $E$   |
|--|----------|------|-------|
| 1. CH <sub>3</sub> NH <sub>2</sub> (+M)=CH <sub>3</sub> +NH <sub>2</sub> (+M)                        | 3.16E+15 | 0    | 85800 |
| Low pressure limit: .48000E+18 .00000E+00 .62618E+02   |          |      |       |
| 2. CH <sub>3</sub> NH <sub>2</sub> +O=CH <sub>2</sub> NH <sub>2</sub> +OH                            | 3.26E+12 | 0    | 1700  |
| 3. CH <sub>3</sub> NH <sub>2</sub> +OH=CH <sub>2</sub> NH <sub>2</sub> +H <sub>2</sub> O             | 3.68E+12 | 0    | -500  |
| 4. CH <sub>3</sub> NH <sub>2</sub> +OH=CH <sub>3</sub> NH+H <sub>2</sub> O                           | 2.46E+12 | 0    | -500  |
| 5. CH <sub>3</sub> NH <sub>2</sub> +O <sub>2</sub> =CH <sub>3</sub> NH+HO <sub>2</sub>               | 8E+12    | 0    | 39000 |
| 6. CH <sub>2</sub> NH <sub>2</sub> +O <sub>2</sub> =H <sub>2</sub> CNH+HO <sub>2</sub>               | 10000000 | 2    | 9200  |
| 7. CH <sub>2</sub> NH <sub>2</sub> +HO <sub>2</sub> =CH <sub>3</sub> NH <sub>2</sub> +O <sub>2</sub> | 10000000 | 2    | 1200  |
| 8. CH <sub>2</sub> NH <sub>2</sub> +O <sub>2</sub> =CH <sub>3</sub> O+HNO                            | 6.00E+12 | 0    | 4000  |
| 9. CH <sub>3</sub> NH+O <sub>2</sub> =H <sub>2</sub> CNH+HO <sub>2</sub>                             | 10000000 | 2    | 6300  |
| 10. CH <sub>3</sub> NH+O <sub>2</sub> =CH <sub>3</sub> O+HNO   | 6E+12    | 0    | 4000  |
| 11. H <sub>2</sub> CNH+O <sub>2</sub> =HCNH+HO <sub>2</sub>  | 3.16E+08 | 2    | 4800  |
| 12. HCNH+O <sub>2</sub> =HCN+HO <sub>2</sub>   | 3.16E+08 | 2    | 4800  |
| 13. H <sub>2</sub> CNNCH <sub>2</sub> =H <sub>2</sub> CN+H <sub>2</sub> CN                           | 3.16E+15 | 0    | -400  |
| 14. OH+CO=H+CO <sub>2</sub>  | 15000000 | 1.3  | -800  |
| Reverse Arrhenius coefficients: 1.68E+09 1.3 21600.0   |          |      |       |
| 15. HO <sub>2</sub> +M=H+O <sub>2</sub> +M   | 2.31E+15 | 0    | 45900 |
| Reverse Arrhenius coefficients: 1.65E+15 .0 -1000.0  |          |      |       |
| N <sub>2</sub> Enhanced by 0   |          |      |       |
| H <sub>2</sub> O Enhanced by 21  |          |      |       |
| CO <sub>2</sub> Enhanced by 5  |          |      |       |
| CO Enhanced by 2   |          |      |       |
| H <sub>2</sub> Enhanced by 3.3   |          |      |       |
| 16. CH <sub>2</sub> O+OH=HCO+H <sub>2</sub> O  | 7.5E+12  | 0    | 200   |
| Reverse Arrhenius coefficients: 2.59E+12 .0 30000.0  |          |      |       |
| 17. CH <sub>3</sub> +O <sub>2</sub> =CH <sub>3</sub> O+O   | 4.8E+13  | 0    | 29000 |
| Reverse Arrhenius coefficients: 3.04E+14 .0 700.0  |          |      |       |
| 18. CH <sub>3</sub> O+M=CH <sub>2</sub> O+H+M  | 3.89E+37 | -6.7 | 33300 |
| Reverse Arrhenius coefficients: 7.71E+32 -6.7 9700.0   |          |      |       |
| 19. CH <sub>3</sub> O+O <sub>2</sub> =CH <sub>2</sub> O+HO <sub>2</sub>                              | 7.6E+10  | 0    | 2700  |
| Reverse Arrhenius coefficients: 1.28E+11 .0 32200.0  |          |      |       |
| 20. CH <sub>3</sub> +HO <sub>2</sub> =CH <sub>4</sub> +O <sub>2</sub>                                | 3.61E+12 | 0    | 0     |
| Reverse Arrhenius coefficients: 4.00E+13 .0 56900.0  |          |      |       |
| 21. HCO+O <sub>2</sub> =CO+HO <sub>2</sub>   | 4.2E+12  | 0    | 0     |

|                                 |                     |             |             |       |  |
|---------------------------------|---------------------|-------------|-------------|-------|--|
| Reverse Arrhenius coefficients: | 7.38E+12            | .0          | 34300.0     |       |  |
| 22.                             | HO2+NO=NO2+OH       | 2.11E+12    | 0           | -500  |  |
| 23.                             | NO2+H=NO+OH         | 3.5E+14     | 0           | 1500  |  |
| 24.                             | NO2+O=NO+O2         | 1E+13       | 0           | 600   |  |
| 25.                             | HNO+OH=NO+H2O       | 3.6E+13     | 0           | 0     |  |
| 26.                             | NH+CO2=HNO+CO       | 10000000    | 2           | 1700  |  |
| 27.                             | NH+O2=NO+OH         | 1300000     | 1.5         | 100   |  |
| 28.                             | NH+NO=N2O+H         | 2.9E+14     | -0.4        | 0     |  |
| 29.                             | NH+NO2=N2O+OH       | 1E+13       | 0           | 0     |  |
| 30.                             | NO+OH(+M)=HONO(+M)  | 2E+12       | 0           | -700  |  |
| Low pressure limit:             | .50000E+24          | -.25100E+01 | -.68000E-01 |       |  |
| N2                              | Enhanced            | by          | 1           |       |  |
| H2O                             | Enhanced            | by          | 5           |       |  |
| 31.                             | HNO+O2=NO+HO2       | 1.00E+13    | 0           | 25000 |  |
| 32.                             | HNO+NO=N2O+OH       | 2E+12       | 0           | 26000 |  |
| 33.                             | HNO+NO2=HONO+NO     | 6E+11       | 0           | 2000  |  |
| 34.                             | HNO+HNO=N2O+H2O     | 4E+12       | 0           | 5000  |  |
| 35.                             | H2NO+H=NH2+OH       | 5E+13       | 0           | 0     |  |
| 36.                             | H2NO+OH=HNO+H2O     | 20000000    | 2           | 1000  |  |
| 37.                             | H2NO+NO=HNO+HNO     | 2.00E+07    | 2           | 13000 |  |
| 38.                             | H2NO+NH2=HNO+NH3    | 3E+12       | 0.00E+00    | 1000  |  |
| 39.                             | HONO+OH=NO2+H2O     | 1.3E+10     | 1           | 100   |  |
| 40.                             | H+O2+N2=HO2+N2      | 6.70E+19    | -1.4        | 0     |  |
| 41.                             | HCO+M=H+CO+M        | 5.12E+21    | -2.1        | 20400 |  |
| Reverse Arrhenius coefficients: | 1.78E+18            | -1.1        | 3000.0      |       |  |
| 42.                             | H2O2+OH=H2O+HO2     | 1.00E+13    | 0           | 1800  |  |
| Reverse Arrhenius coefficients: | 2.80E+13            | .0          | 32800.0     |       |  |
| 43.                             | HCO+HO2=CH2O+O2     | 1E+14       | 0           | 3000  |  |
| Reverse Arrhenius coefficients: | 3.66E+15            | .0          | 46000.0     |       |  |
| 44.                             | H+HO2=OH+OH         | 2.50E+14    | 0           | 1900  |  |
| Reverse Arrhenius coefficients: | 1.20E+13            | .0          | 40100.0     |       |  |
| 45.                             | H2O2+O2=HO2+HO2     | 4.46E+12    | 0           | 39500 |  |
| Reverse Arrhenius coefficients: | 3.02E+12            | .0          | 1400.0      |       |  |
| 46.                             | H2O2+M=OH+OH+M      | 6.00E+16    | 0           | 45500 |  |
| Reverse Arrhenius coefficients: | 4.55E+14            | .0          | -5100.0     |       |  |
| N2                              | Enhanced            | by          | 1           |       |  |
| H2O                             | Enhanced            | by          | 7           |       |  |
| 47.                             | H2CN+M=HCN+H+M      | 3E+14       | 0.00E+00    | 22000 |  |
| 48.                             | HCO+NO2=H+CO2+NO    | 8.40E+15    | -0.8        | 1900  |  |
| 49.                             | CH3NH2+O=CH3NH+OH   | 2.17E+12    | 0           | 1700  |  |
| 50.                             | CH3NH2+M=CH2NH2+H+M | 2.00E+17    | 0           | 88400 |  |
| 51.                             | CH3NHOH=CH4+HNO     | 6E+12       | 0           | 0     |  |
| 52.                             | H+O2=OH+O           | 5.13E+16    | -0.8        | 16500 |  |

|                                 |          |    |          |          |       |
|---------------------------------|----------|----|----------|----------|-------|
| Reverse Arrhenius coefficients: | 1.31E+13 | .0 | 700.0    |          |       |
| 53. O+H2O=OH+OH                 |          |    | 6.8E+13  | 0        | 18400 |
| Reverse Arrhenius coefficients: | 6.30E+12 | .0 | 1100.0   |          |       |
| 54. H+H2O=OH+H2                 |          |    | 9.50E+13 | 0        | 20300 |
| Reverse Arrhenius coefficients: | 2.20E+13 | .0 | 5100.0   |          |       |
| 55. OH+HO2=H2O+O2               |          |    | 5E+13    | 0        | 1000  |
| Reverse Arrhenius coefficients: | 6.33E+14 | .0 | 73900.0  |          |       |
| 56. NH3+OH=NH2+H2O              |          |    | 2040000  | 2        | 600   |
| 57. NH3+H=NH2+H2                |          |    | 636000   | 2.40E+00 | 10200 |
| 58. CN+H2O=HCN+OH               |          |    | 8E+12    | 0        | 7500  |
| 59. CN+O2=NCO+O                 |          |    | 7.5E+12  | 0        | -400  |
| 60. NCO+NO2=CO+NO+NO            |          |    | 1.3E+13  | 0        | 0     |
| 61. NCO+NO2=CO2+N2O             |          |    | 5.4E+12  | 0        | 0     |
| 62. H2NO+O=NH2+O2               |          |    | 4E+13    | 0        | 0     |
| 63. NH2+NO2=N2O+H2O             |          |    | 3.20E+18 | -2.2     | 0     |
| 64. NH2+NO=N2+H2O               |          |    | 1.30E+16 | -1.3     | 0     |
| 65. NH+O2=HNO+O                 |          |    | 460000   | 2        | 6500  |
| 66. NH+NO=N2+OH                 |          |    | 2.2E+13  | -0.2     | 0     |
| 67. HNO+H=H2+NO                 |          |    | 4.4E+11  | 0.7      | 700   |
| Reverse Arrhenius coefficients: | 1.50E+13 | .0 | 52000.0  |          |       |

A similar rate of production analysis was performed, but only considering the most important outlet species (HCN, NO, NO<sub>2</sub>, NH<sub>3</sub> and N<sub>2</sub>O). A further reduction of the mechanism was achieved. The reaction tree of the further reduced mechanism (FRM) is shown in **Figure 30**. The FRM consists of only 18 reactions and 21 species as shown in **Table 8**, which presents a significant reduction in comparison to the detailed mechanism. A further analysis with adjustment of the reaction rate constant (where *A*, *m* and *E* are adjusted) was not attempted, since that it would produce a mechanism with empirical reaction rate constants.

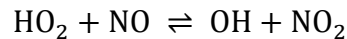


### 3.7 Simulation Comparison of Alternative Reagents for NO<sub>x</sub>

#### Reduction

A comparison was performed in terms of NO<sub>x</sub> reduction performance for MMA, urea, CYA and ammonium sulfate. The RM for MMA, a chemical kinetics scheme developed by the Lehigh University Energy Research Center (ERC) for urea and CYA, and Chen et al.'s [35] mechanism for ammonium sulfate, were used in the simulation comparison. The inlet conditions used for the simulation were: 1.0 atm, temperature from 600 K to 1400K, molar concentrations for: [CO] = 0.001, [CO<sub>2</sub>] = 4.12, [NO] = 0.01, [O<sub>2</sub>] = 11.75, [H<sub>2</sub>O] = 9.95; and NSR = 1. The results of the simulation are included in **Figures 31 to 33**.

The comparison results in **Figure 31** show that an MMA-based SNCR NO<sub>x</sub> reduction process has the great advantage of reducing NO at much lower temperatures than the other reagents. MMA works best at injection temperatures around 700 K, as compared to the other reagents that work at around 1100 K. This implies that MMA could be injected after the convective tube bank sections in utility boilers, where flow is more homogenous and there is easier access for the injection lances. Additionally, the temperature window of MMA is comparatively wider than the windows for the other tested reagents. However, the production of NO<sub>2</sub> from MMA model is significantly larger, while the other reagents have only relatively negligible NO<sub>2</sub> formation. This can possibly result from the following reaction:



Excess HO<sub>2</sub> is generated by the below pathway of CH<sub>3</sub>NH<sub>2</sub> decomposition:



This is supported from studies by Miller and Bowman [43] that report that the primary product of the  $\text{H}_2\text{O}_2 + \text{NH}_3$  (note that  $\text{H}_2\text{O}_2$  becomes  $\text{HO}_2$  during the reaction process) reaction would be  $\text{NO}_2$  rather than  $\text{N}_2$  at lower temperatures. The overall  $\text{NO}_x$  reduction efficiency of MMA seems to be hampered by the production of  $\text{NO}_2$ . Nevertheless, additional studies are needed on  $\text{NO}_2$  production and how to tune its production down, because experimental studies by Nakanishi et al. [49] for example, indicate that high NO reduction can be obtained at low temperatures (around 695 K) avoiding that the reaction which generates  $\text{NO}_2$  from NO influence the chemical reduction process. In regard to  $\text{NH}_3$  slip, the slips for all four investigated reagents were acceptable since that they all fall below the 5 ppm level, at maximum reduction conditions. However, for MMA, the  $\text{NH}_3$  level is below 5 ppm for the entire temperature range, which indicates that  $\text{NH}_3$  slip is not an issue when using MMA as a reagent in the SNCR  $\text{NO}_x$  reduction process. HCN can become an issue with MMA systems and a mitigation method for HCN needs to be further explored.

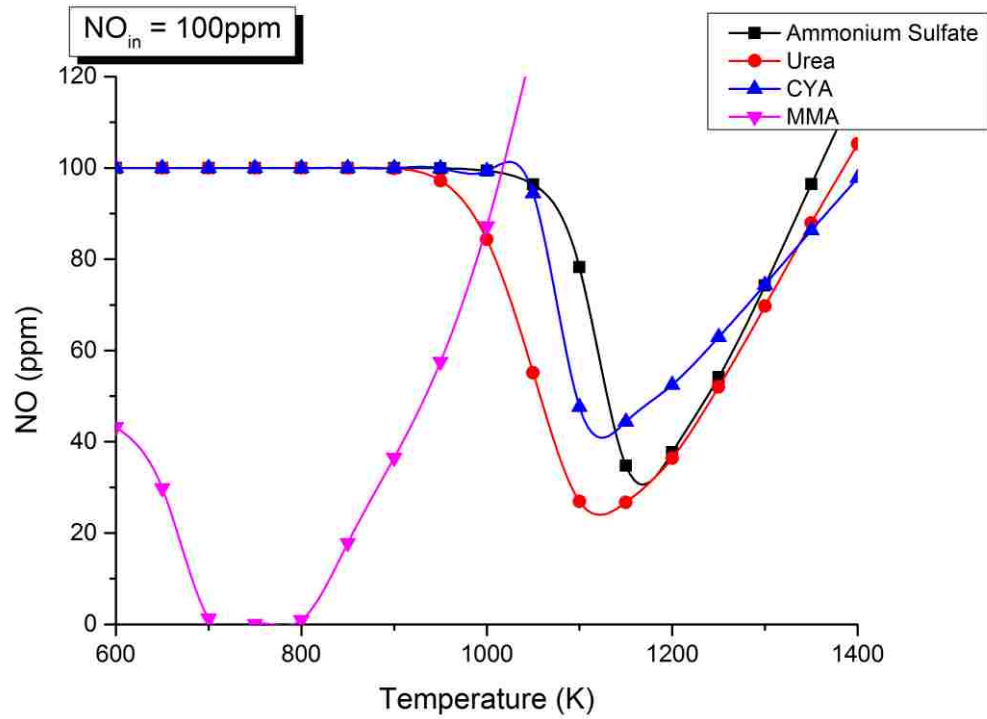


**Figure 31.** Predictions of outlet NO concentration using different reagents predicted by corresponding kinetics model.

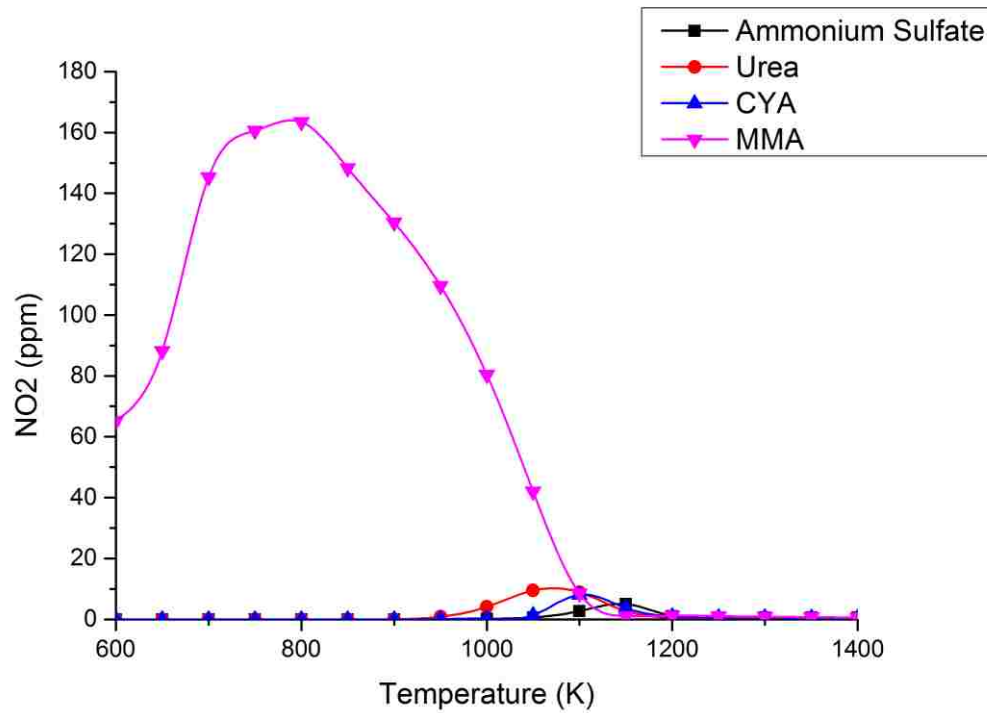


**Figure 32.** Predictions of outlet NO<sub>2</sub> concentration using different reagents predicted by corresponding kinetics model.

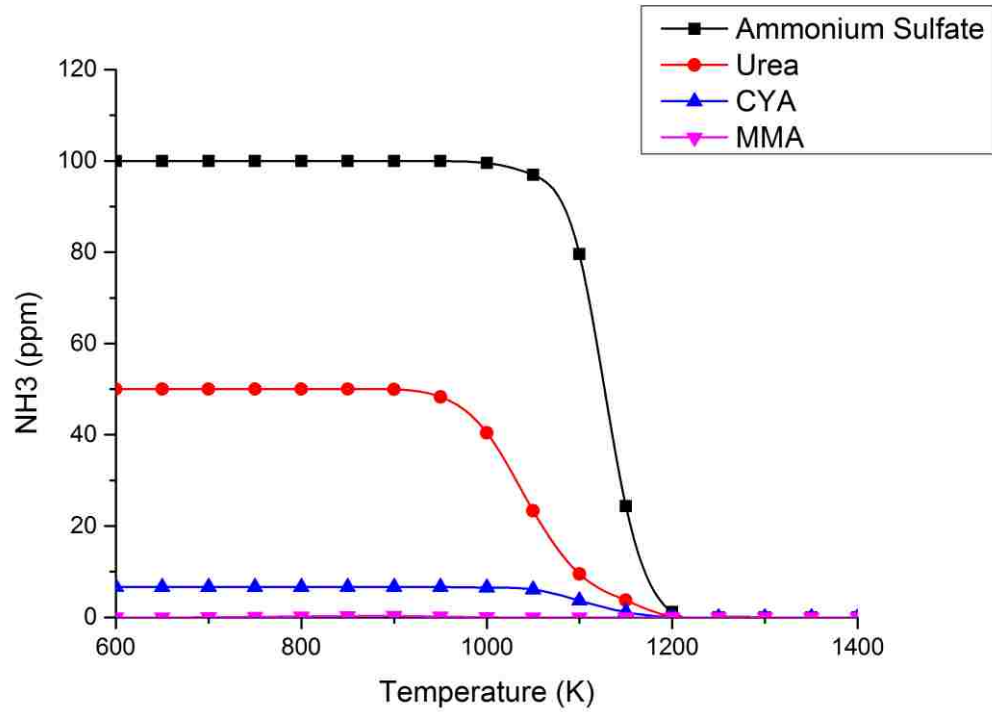


**Figure 33.** Predictions of Outlet  $\text{NH}_3$  concentration using different reagents predicted by corresponding kinetics model.

According to the above comparisons and the previous discussions, the design of an MMA-based SNCR system would be similar to a conventional SNCR system, except for the injection location, due to the different optimal reaction temperatures of a MMA-based SNCR process. The form of MMA is expected to be aqueous. As previously mentioned, the injection points of MMA-based SNCR should be placed at areas where the temperatures are around 700 K – 800 K, which are most likely locations near the economizer in most CFPPs.

## **Chapter IV – Opportunities for Monomethylamine-Based SNCR in Other Industrial Applications**

### **4.1 Introduction**

The chemical kinetics simulation results of this study illustrate that MMA has great advantages as a reagent for SNCR systems, working at relatively low temperatures in the range from 700 K to 850 K. This provides additional opportunities for the potential of applying the MMA process to other industrial applications. Modeling of a gas turbine was performed, using the reduced MMA kinetics mechanism model developed in this study. This application is associated with relatively lower flue gas temperatures than are experiencing in coal-fired units.

### **4.2 Gas Turbine Simulation**

The objective of this simulation is to predict NO reduction performance and reagent consumption of a MMA-based SNCR NO<sub>x</sub> reduction system for a 42 MW natural gas turbine plant. One major reason for estimating the reagent consumption of the MMA-based SNCR system is that, in general, the price of MMA is higher than that of conventional reagents like NH<sub>3</sub> and urea, the estimation of MMA usage is then valuable for analyzing the cost-effectiveness of MMA-based SNCR systems in comparison to other conventional SNCR systems. Another reason for doing such modeling is that the temperatures of exhaust gases in the gas turbine outlet duct are usually below 850 K, which means that conventional reagent-based SNCR NO<sub>x</sub> control systems have difficulties to perform as required under such temperature conditions. Typically, catalysis systems (selective catalytic reduction)

are retrofit in gas turbine plants, which results in increased operating and maintenance costs. Using a novel MMA SNCR system in gas turbines seems to have merit, and motivates the an expansion of the present study to explore this option theoretically.

The dimensions of a typical facility are attached in **Figure 34**. Assuming a flue gas flow velocity and a linear temperature distribution along the flow path, a PFR model was used to treat the physical problem. A target for NO<sub>x</sub> removal of 25% was set for the simulations. Simulations where performed with the gas turbine working on an open cycle (no combined cycle). The inlet temperature of the flue gases into the PFR model was set at 823 K. The outlet temperature was set at 623 K. The gas flow rate for this typical unit is 217 m<sup>3</sup>/s. The suggested flow gas path way is shown in **Figure 35**. Following the above conditions and assumptions, the following calculations were performed:

The length of AB:

$$h = 51.857 - 32.639 = 19.218 \text{ m} \quad \text{Eq. 7}$$

The length of BC:

$$l = 5.105 + 2.873 + 3.010 = 10.988 \text{ m} \quad \text{Eq. 8}$$

Total approximate flow path way length:

$$L = l + h = 30.206 \text{ m} \quad \text{Eq. 9}$$

Average radius of the path way:

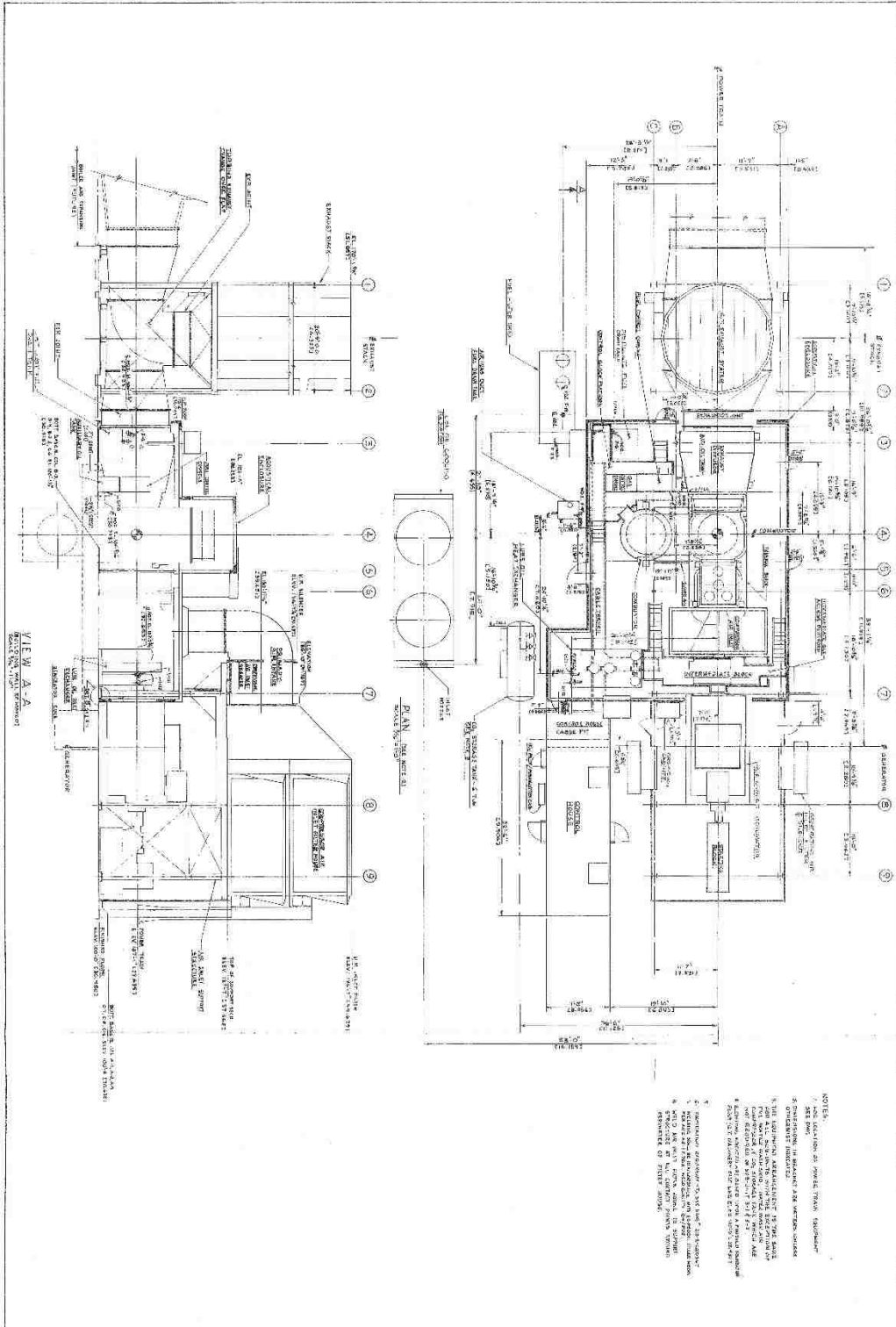
$$r = 3.010 \times \frac{19.218}{30.200} + 2.24 \times \frac{10.988}{30.200} = 2.730 \text{ m} \quad \text{Eq. 10}$$

Maximum residence time:

$$t_{max} = \frac{(2.730\text{m})^2 \times \pi \times 30.206}{217 \text{ m}^3/\text{s}} = 3.20 \text{ s} \quad \text{Eq. 11}$$

Estimated temperature slope along the path way:

$$\Delta T = \frac{550^{\circ}\text{C} - 350^{\circ}\text{C}}{3.20\text{s}} = 62.5 \text{ }^{\circ}\text{C}/\text{s} = 62.5 \text{ K}/\text{s} \quad \text{Eq. 12}$$



620362 — PLANT LAYOUT  
(SHEET 1 OF 2)

Figure 34. Combined cycle unit diagram.

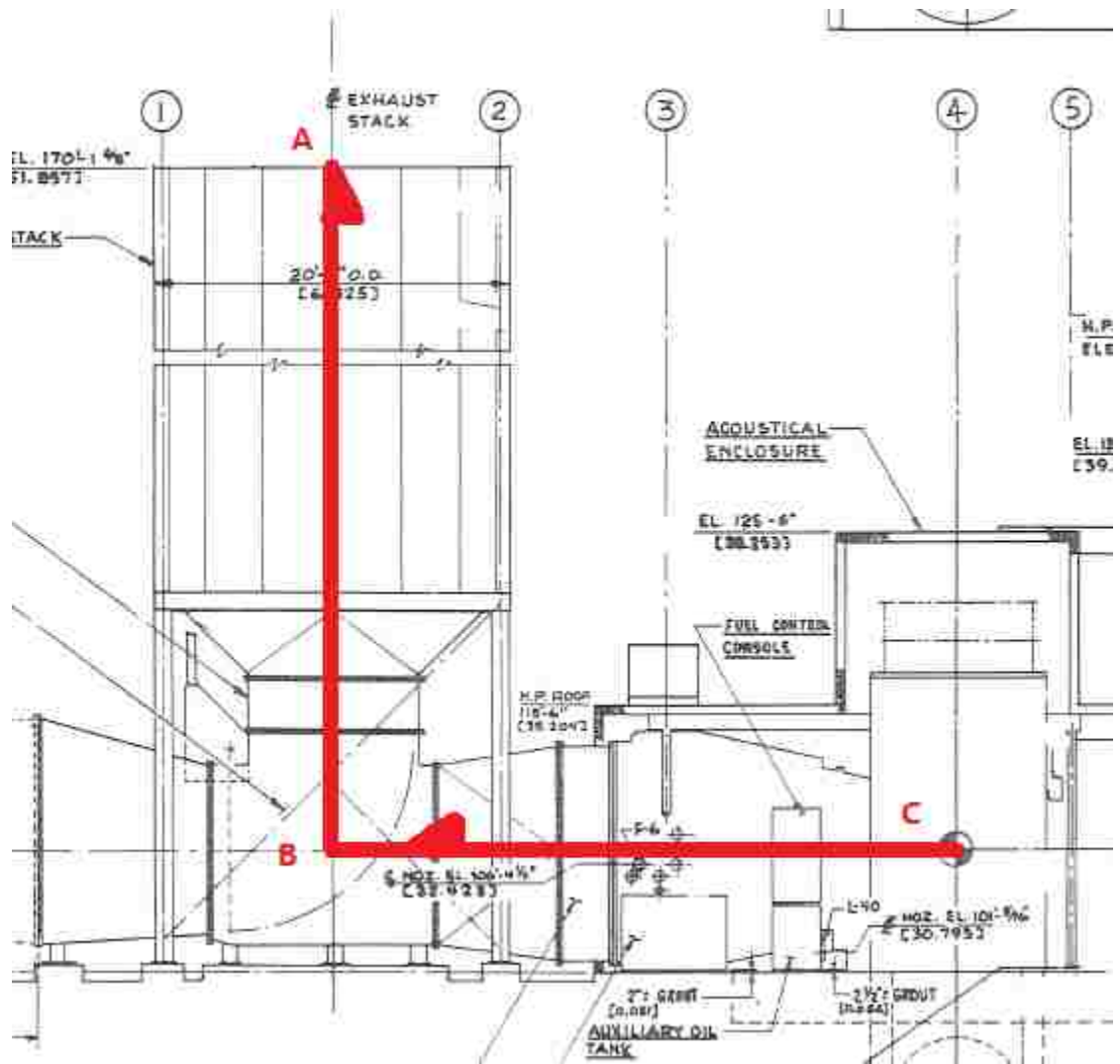


Figure 35. Modeled ideal path way of flue gases.

Initial conditions of the inlet gases used in the simulations (by volume):

H<sub>2</sub>O = 9.95 %

O<sub>2</sub> = 11.75 %

CO = 500 ppm

CO<sub>2</sub> = 4.12 %

NO = 800 ppm

N<sub>2</sub> = balance

(typical from conventional natural gas turbines without low-NO<sub>x</sub> technology)

NO<sub>x</sub> reduction results at different NSRs are included in **Figure 36**. Thus to achieve NO reductions greater than the expected 25% target, NSRs in excess of 0.5 are required at inlet temperatures below 725 K. The NH<sub>3</sub> slip expected with these conditions is below 5 ppm (see **Figure 37**).

Depending on the NSR in excess of 0.5 and the temperature below 725 K chosen, the HCN emissions from the process could be as high as 5 ppm, with lower HCN values as injection occurs at lower temperatures (see **Figure 38**). To limit MMA slip at the lowest values possible, the NSRs should be at the minimum possible to achieve the required 25% NO reduction (see **Figure 39**).

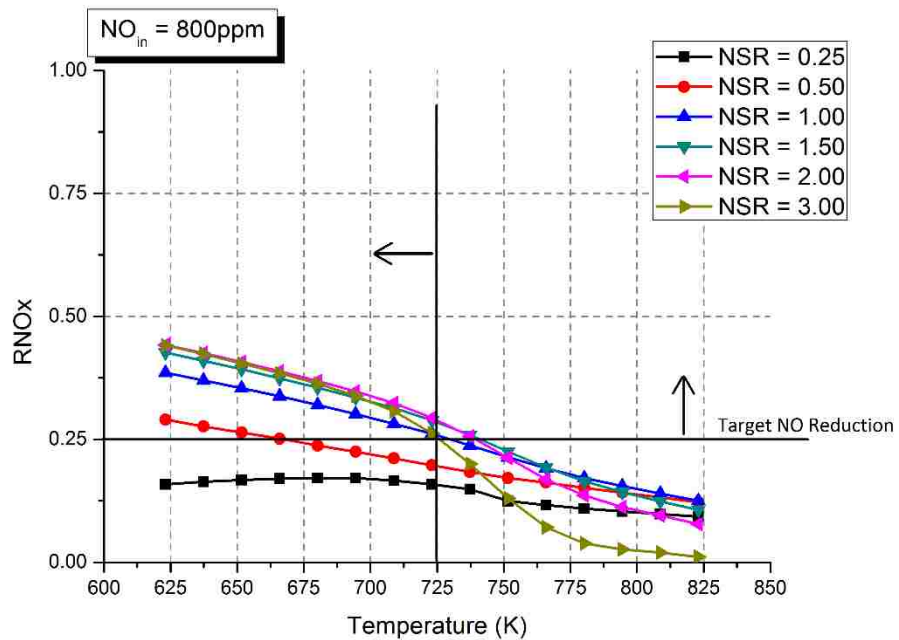


**Figure 36.** NO<sub>x</sub> reduction vs. temperature at various NSRs.

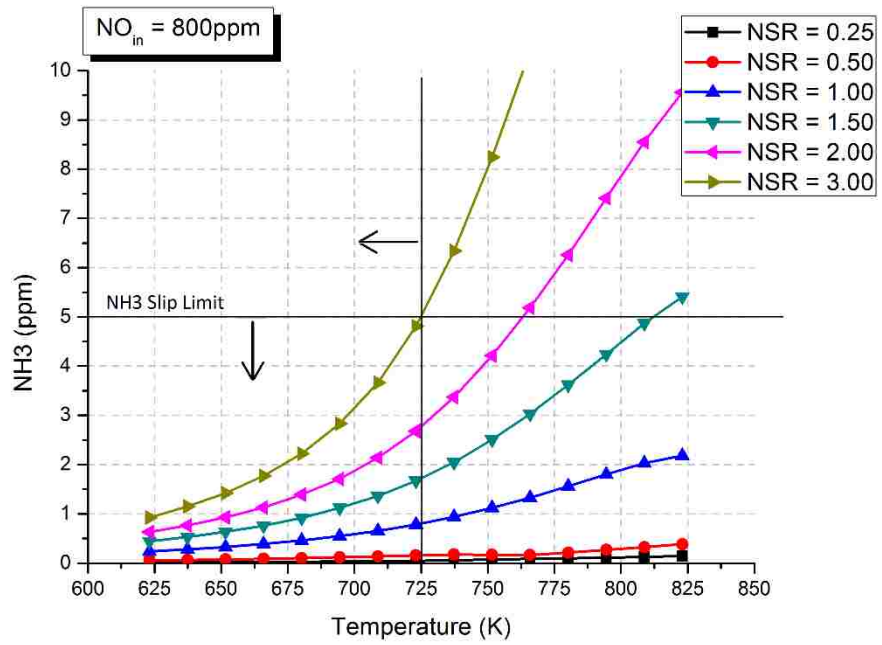


Figure 37. NH<sub>3</sub> slip vs. temperature at various NSRs.

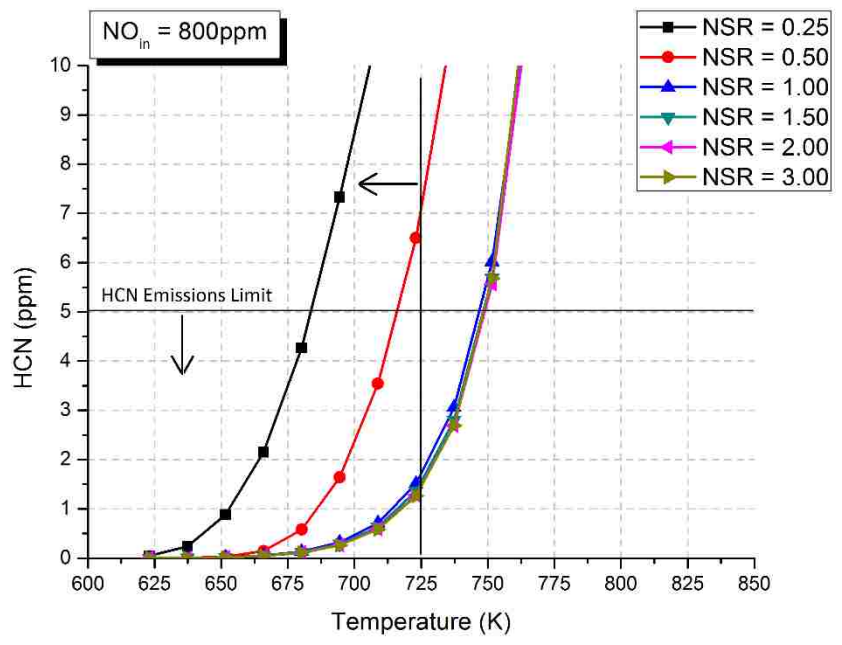
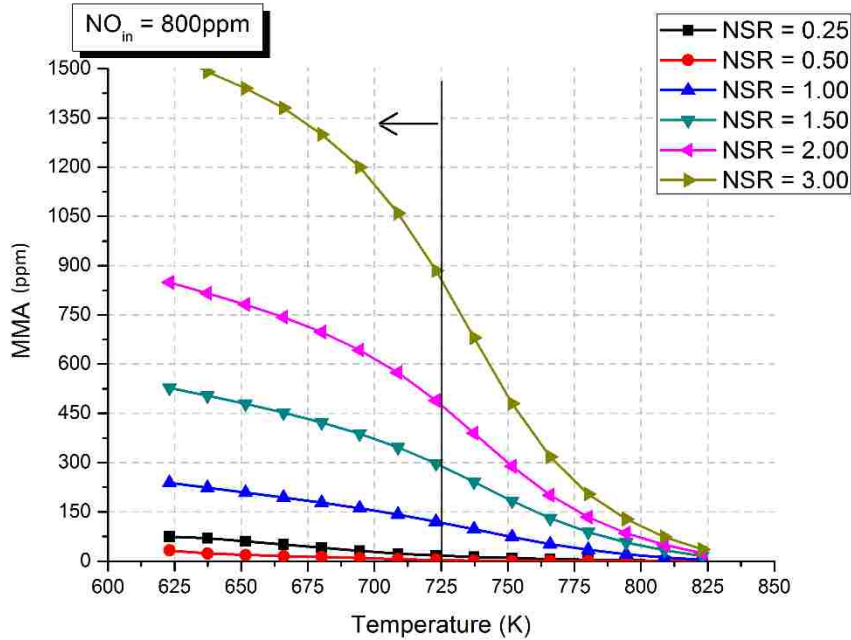


Figure 38. HCN production vs. temperature at various NSRs.



**Figure 39.** Unreacted MMA vs. temperature at various NSRs.

In summary, the simulation results indicate that to achieve 25% NO reduction, the MMA injection NSR should be at least around 0.5 and the injection point should be located 22.4 m away from the exhaust duct inlet (point C on **Figure 35**), where the temperature is around 675 K. To inject the MMA with a NSR = 0.5 at the point mentioned above is the best choice because it requires minimum MMA consumption while achieving the target NO removal. The overall usage of MMA at the mentioned design point is presented in **Table 9**.

**Table 9.** MMA consumption under best operating condition.

| Description                       |  |                   | Single Zone<br>NSR = 0.5 |
|-----------------------------------|--|-------------------|--------------------------|
| <b>Load</b>                       |  | <b>UNITS</b>      | <b>42 MW</b>             |
| <b>FACILITY/BOILER</b>            |  |                   |                          |
| Unit Type                         |  | -                 | GT                       |
| Unit Rating                       |  | MW                | 42                       |
| Heat Rate assumed                 |  | BTU/kW-hr         | 13,000                   |
| Heat Input                        |  | kW                | 160017                   |
| Excess Air                        |  | %                 | 12                       |
| Gas flow assumed                  |  | wet               | kg/hr                    |
|                                   |  | dry               | kg/hr                    |
| (1 atm, 273 K)                    |  | wet               | Nm <sup>3</sup> /hr      |
|                                   |  | dry               | DNm <sup>3</sup> /hr     |
| NO <sub>x</sub>                   |  | kg/hr             | 433.42                   |
|                                   |  | ppmv              | 800.4                    |
| <b>MMA DESIGN</b>                 |  |                   |                          |
| <b>MMA consumption</b>            |  |                   |                          |
| MMA solution strength             |  | % wt              | 40                       |
| MMA 40 % aqueous density at 275 K |  | kg/m <sup>3</sup> | 909.5                    |
| MMA anhydrous density at 295 K    |  | kg/m <sup>3</sup> | 1.3                      |
| Air density at 295 K              |  | kg/m <sup>3</sup> | 1.2                      |
| <b>ZONE 1</b>                     |  |                   |                          |
| NO <sub>x</sub> inlet             |  | kg/hr             | 433.6                    |
| NO <sub>x</sub> reduction         |  | %                 | 25                       |
| NO <sub>x</sub> outlet            |  | kg/hr             | 325.2                    |
| NO <sub>x</sub> removed           |  | kg/hr             | 108.4                    |
| NSR                               |  | mol/mol           | 0.5                      |
| <b>MMA consumption</b>            |  | anhydrous         | kg/hr                    |
| aqueous (MMA + water)             |  | <b>40%</b>        | kg/hr                    |
|                                   |  | liters/hr         | 615.5                    |

The 2005 price of anhydrous MMA is around \$0.72 per pound (\$1.59 per kilogram) [65]. Recent increases in MMA price has been of about \$0.13 per pound (\$0.28 per kilogram) [66, 67]. Assuming a list price of anhydrous MMA at \$1.87 per kilogram, the

reagent cost for the example of this section is \$437.4 per hour. Assuming a comparable urea-based SNCR system can be applied to the above gas turbine example and a price of commercial grade urea of is \$0.15 per kilogram [68], using the results of reagent utilization tests reported by Staudt et al. [69], that the urea utilization rate at 25% NO<sub>x</sub> reduction and 0.46 NSR condition is 56%, then the usage of urea is 348.4 kg/hr and the reagent cost for the urea-based SNCR system is \$52.3 per hour. It's obvious that the reagent consumption cost of a MMA-based SNCR system is greater than that of urea-based SNCR system. However, utilization of a urea-based SNCR NO<sub>x</sub> reduction system in a gas turbine is prohibited by the relatively low temperatures of the flue gas (which would result in excessive NH<sub>3</sub> slip). Hence, MMA offers an alternative to NO<sub>x</sub> control for gas turbines, where conventional SNCR system is not suited for and SCR is a more expensive proposition.

## Chapter V – Conclusions and Recommendations

The objective of this thesis was to study MMA as an alternative reagent for SNCR NO<sub>x</sub> reduction systems. This was accomplished by performing a literature review, chemical kinetics mechanism research and kinetics simulations in order to find the potential advantages of using MMA over other traditional and alternative reagents. The study also attempted to propose a reduced chemical kinetics model for simulating MMA-based NO<sub>x</sub> abatement systems. The study was also extended to discuss the possibility of MMA-based SNCR systems in full-scale fuel combustion devices, especially for units whose operating flue gas temperatures are under 850 K and require strict NH<sub>3</sub> emissions control.

Based on the result of the study, the following conclusions are made:

- (1) Traditional SNCR NO<sub>x</sub> systems, which use conventional reagents such as NH<sub>3</sub> and urea, have limitations in controlling NO<sub>x</sub> emissions at low temperatures (below 800 K). Additionally, narrow reaction temperature windows for conventional reagents in SNCR systems result in difficulties in maintaining plant generating availability, due to NH<sub>3</sub> slip problems. Meanwhile, previous researches have shown that MMA could be an alternative reagent for SNCR NO<sub>x</sub> systems, which has merit to be used at relatively low gas temperatures in SNCR systems.
- (2) A chemical kinetics model was assembled, based on the kinetics scheme by Kantak et al. [60], comprising 350 reactions and 65 species. This detailed mechanism was reduced in this study to 67 reactions and 36 species, without greatly sacrificing the prediction accuracy of the model. The proposed model was validated with experimental data obtained in the temperature range from 770 K to

900 K. A further reduced kinetics mechanism, which has only 18 reactions and 21 species, was also proposed, but reaction rate adjustment would be required for this reduced scheme to provide very good agreement with results from the original mechanism. A sensitive analysis of the reduced kinetics model and a simulation comparison with other reagents under identical process conditions suggest that the MMA mechanism is very sensitive to the concentration of CO in the flue gas, which can shift the optimal temperatures downward to less than 600 K and it has superior NO reduction performance at temperatures below 900 K, when compared to other conventional SNCR reagents.

- (3) An example modeling of a gas turbine was performed using the reduced MMA mechanism. The modeling results show that a MMA-based SNCR system would be capable of achieving a target NO reduction of 25% with reasonable reagent usage (NSR = 0.5), and such system would not suffer from the typical drawbacks associated with conventional SNCR systems when applied to gas turbines.

The following recommendations are provided:

- (1) It is suggested to perform additional theoretical studies in order to fully understand the MMA-NO chemistry, and the mechanism of NO<sub>2</sub> and HCN formation in the low temperature MMA-based NO<sub>x</sub> reduction process. It could be that the reaction,  $\text{HO}_2 + \text{NO} \rightleftharpoons \text{OH} + \text{NO}_2$ , plays a significant role in the MMA chemical process, or that above reaction is overrated in the kinetic model, which is supported by Nakanishi et al. [49].
- (2) It is recommended to perform experimental MMA testing in laboratory and pilot-scale apparatus to better evaluate the performance and associated problems of

MMA when used in a SNCR process. The potential of using MMA in natural gas combined cycle plant has a lot merit and needs to be fully validated in appropriate field tests.

## References

- [1] Kitto, J. B., and Stultz, S. C., 2005, *Steam: It is Generation and Use*. Barberton: The Babcock & Wilcox Company.
- [2] *NO<sub>x</sub>: How nitrogen oxides affect the way we live and breathe*, 1998, Office of Air Quality Planning and Standards Research, Triangle Park, NC.
- [3] *1970 - 2012 Average annual emissions, all criteria pollutants in MS Excel*, 2013, U.S. Environmental Protection Agency, Washington, DC.
- [4] *The Annual Energy Outlook 2013*, 2013, U.S. Energy Information Administration, Washington, DC.
- [5] Miller, P. J., and Van Atten, C., 2004, *North American power plant emissions*, Commission for Environmental Cooperation of North America, Montreal, PQ, Canada.
- [6] Zeldovich, Y. B., 1946, "The oxidation of nitrogen in combustion and explosions," *Acta Physicochimica URSS*, 21(4), pp. 577-628.
- [7] Fenimore, C. P., 1971, December, "Formation of Nitric Oxide in Premixed Hydrocarbon Flames," *Symposium (International) on Combustion*, **Vol.** 13, pp. 373-380.
- [8] Poole, D. R., and Graven, W. M., 1961, "Kinetics of the Reaction of Ammonia and Nitric Oxide in the Region of Spontaneous Ignition<sup>1</sup>," *Journal of the American Chemical Society*, 83(2), pp.283-286.
- [9] Beychok, M. R., 1973, "NO<sub>x</sub> Emission from Fuel Combustion Controlled," *The Oil and Gas Journal*, pp, 53-56.
- [10] Lyon, R. K., 1975, "Method for the Reduction of the Concentration of No in Combustion Effluents Using Ammonia." U.S. Patent 3900554 A.
- [11] Arand, J. K., Muzio, L.J., and Sotter, J. G., 1980, "Urea reduction of NO<sub>x</sub> in Combustion Effluents." U.S. Patent 4208386.
- [12] Tayyeb Javed, M., Irfan, N., and Gibbs, B. M., 2007, "Control of Combustion-Generated Nitrogen Oxides by Selective Non-catalytic Reduction," *Journal of Environmental Management*, 83(3), pp. 251-289.

- [13] Zandaryaa, S., Gavasci, R., Lombardi, F., and Fiore, A., 2001, "Nitrogen Oxides from Waste Incineration: Control by Selective Non-catalytic Reduction," *Chemosphere*, **42**(5), pp. 491-497.
- [14] Poole, D. R., and Graven, W. M., 1961, "Kinetics of the Reaction of Ammonia and Nitric Oxide in the Region of Spontaneous Ignition<sup>1</sup>," *Journal of the American Chemical Society*, **83**(2), pp. 283-286.
- [15] Wise, H., and Frech, M. F., 2004, "Kinetics of Oxidation of Ammonia by Nitric Oxide," *The Journal of Chemical Physics*, **22**(8), pp. 1463-1464.
- [16] Lee, G. W., Shon, B. H., Yoo, J. G., Jung, J. H., and Oh, K. J., 2008, "The Influence of Mixing between NH<sub>3</sub> and NO for a De-NO<sub>x</sub> Reaction in the SNCR Process," *Journal of Industrial and Engineering Chemistry*, **14**(4), pp. 457-467.
- [17] Muzio, L. J., Arand, J. K., and Teixeira, D. P., 1977, December, "Gas phase decomposition of nitric oxide in combustion products," *Symposium (International) on Combustion*, **Vol. 16**, pp. 199-208.
- [18] Azuhata, S., Akimoto, H., and Hishinuma, Y., 1985, "The Behavior of Nitrogen Oxides in the N<sub>2</sub>H<sub>4</sub>-NO-O<sub>2</sub> Reaction," *AIChE journal*, **31**(7), pp. 1223-1225.
- [19] Wenli, D., Dam-Johansen, K., and Østergaard, K., 1991, December, "Widening the Temperature Range of the Thermal DeNO<sub>x</sub> Process. An Experimental Investigation," *Symposium (International) on Combustion*, **Vol. 23**, pp. 297-303.
- [20] Bae, S. W., Roh, S. A., and Kim, S. D., 2006, "NO Removal by Reducing Agents and Additives in the Selective Non-catalytic Reduction (SNCR) Process," *Chemosphere*, **65**(1), pp. 170-175.
- [21] Lyon, R. K., and Longwell, J. P., 1976, February, "Selective Non-catalytic Reduction of NO<sub>x</sub> by NH<sub>3</sub>," *EPRI NO<sub>x</sub> Control Technology Seminar*, San Francisco, California.
- [22] Lyon, R. K., 1987, "Thermal DeNO<sub>x</sub> Controlling Nitrogen Oxides Emissions by a Noncatalytic Process," *Environmental science & technology*, **21**(3), pp. 231-236.
- [23] Muzio, L.J., Arand, J.K., Maloney, K.L., 1978a. "Non-catalytic NO<sub>x</sub> Removal with NH<sub>3</sub>," Exxon/EPRI Report FP-735, KVB Inc. Tustin, CA.

- [24] Muzio, L. J., Maloney, K. L., and Arand, J. K., 1979, December. "Reactions of NH<sub>3</sub> with NO in Coal-derived Combustion Products," *Symposium (International) on Combustion*, **Vol. 17**, pp. 89-96.
- [25] Azuhata, S., Akimoto, H., and Hishinuma, Y., 1982, "Effect of H<sub>2</sub>O<sub>2</sub> on Homogeneous Gas Phase NO Reduction Reaction with NH<sub>3</sub>," *AIChE Journal*, **28**(1), pp. 7-11.
- [26] Lodder, P., and Lefers, J. B., 1985, "Effect of Natural gas, C<sub>2</sub>H<sub>6</sub> and CO on the Homogeneous Gas Phase Reduction of NO<sub>x</sub> by NH<sub>3</sub>," *The Chemical Engineering Journal*, **30**(3), pp. 161-167.
- [27] Wenli, D., Dam-Johansen, K., and Østergaard, K., 1989, "The Influence of Additives on Selective Non-catalytic Reduction of Nitric Oxide with NH<sub>3</sub>," *ACHEMASIA*, Beijing, P. R. China.
- [28] Leckner, B., Karlsson, M., Dam-Johansen, K., Weinell, C. E., Kilpinen, P., and Hupa, M., 1991, "Influence of Additives on Selective Noncatalytic Reduction of Nitric Oxide with Ammonia in Circulating Fluidized Bed Boilers," *Industrial & engineering chemistry research*, **30**(11), pp. 2396-2404.
- [29] Robin, M. A. I., Price, H. J., and Squires, R. T., 1991, "Tailoring NH<sub>3</sub> Based SNCR for Installation on Power Plants Boilers," *Joint EPA/EPRI Symposium on Stationary Combustion NOx Control*, **Vol. 118**, Springfield, VA.
- [30] Teixeira, D. P., Muzio, L. J., and Montgomery, T. A., 1991, October, "Effect of trace combustion species on SNCR performance," *AFRC/JFRC International Conference on Environmental Control of Combustion Processes*, Honolulu, HI.
- [31] Teixeira, D. P., and Muzio, L. J., 1991, "N<sub>2</sub>O emission from SNCR processes," *First International Conference on Combustion Technologies for Clean Environment*, Vica Mourta (Alcrave) Portugal, pp. 9-14.
- [32] Teixeira, D., Muzio, L. J., Montgomery, T. A., Quartucy, G. C., and Martz, T. D., 1991, November, "Widening the Urea Temperature Window," *Proceedings of 1991 Joint Symposium on Stationary Combustion NOX Control*, NTIS.
- [33] Hemberger, R., Muris, S., Pleban, K. U., and Wolfrum, J., 1994, "An Experimental and Modeling Study of the Selective Noncatalytic Reduction of NO by

- Ammonia in the Presence of Hydrocarbons.” *Combustion and Flame*, **99**(3), pp. 660-668.
- [34] Salimian, S., and Hanson, R. K., 1980, “A Kinetic Study of NO Removal from Combustion Gases by Injection of NHi-Containing Compounds,” *Combustion Science and Technology*, **23**(5-6), pp. 225-230.
- [35] Chen, S. L., Cole, J. A., Heap, M. P., Kramlich, J. C., McCarthy, J. M., and Pershing, D. W., 1989, December, “Advanced NO<sub>x</sub> Reduction Processes Using-NH and-CN Compounds in Conjunction with Staged Air Addition,” *Symposium (International) on Combustion*, **Vol. 22**, pp. 1135-1145.
- [36] Jodal, M., Nielsen, C., Hulgaard, T., and Dam-Johansen, K., 1989, “A Comparative Study of Ammonia and Urea as Reductants in Selective Non-Catalytic Reduction of Nitric Oxide,” *Achemasia*, Beijing, P. R. China.
- [37] Jones, D. G., Muzio, L. J., Stocker, E., Basel, M., Nuesch, P. C., Negrea, S., Lautenschlager, G., and Rose, G., 1989, “Two-Stage DeNO<sub>x</sub> Process Test Data for 300 TPD MSW Incineration Plant,” *Air & Waste Management Assoc.*, Pittsburgh, PA.
- [38] Lee, J. B., and Kim, S. D., 1996, “Kinetics of NO<sub>x</sub> Reduction by Urea Solution in a Pilot Scale Reactor,” *Journal of chemical engineering of Japan*, **29**(4), pp. 620-626.
- [39] Rota, R., and Zanoelo, E. F., 2003, “Influence of Oxygenated Additives on the NO<sub>x</sub>OUT Process Efficiency,” *Fuel*, **82**(7), pp. 765-770.
- [40] Perry, R. A., and Siebers, D. L., 1986, “Rapid Reduction of Nitrogen Oxides in Exhaust Gas Streams,” *Nature*, **324**(6098), pp. 657-658.
- [41] Perry, R. A., 1988, "NO Reduction Using Sublimation of Cyanuric Acid," U.S. Patent 4731231.
- [42] Caton, J. A., and Siebers, D. L., 1989, “Comparison of Nitric Oxide Removal by Cyanuric Acid and By Ammonia,” *Combustion Science and Technology*, **65**(4-6), pp. 277-293.
- [43] Miller, J. A., and Bowman, C. T., 1989, “Mechanism and Modeling of Nitrogen Chemistry in Combustion,” *Progress in Energy and Combustion Science*, **15**(4), pp. 287-338.

- [44] Streichsbier, M., Dibble, R. W., and Perry, R. A., 1998, "Non-Catalytic NO<sub>x</sub> Removal from Gas Turbine Exhaust with Cyanuric Acid in a Recirculating Reactor," Ph.D. Dissertation, University of California, Berkeley.
- [45] Jolley, L. J., 1934, "The Thermal Oxidation Of Methylamine," *Journal of the Chemical Society (Resumed)*, pp. 1957-1966.
- [46] Emeléus, H. J., and Jolley, L. J., 1935, "Kinetics Of The Thermal Decomposition of Methylamine," *Journal of the Chemical Society (Resumed)*, pp. 929-935.
- [47] Dorko, E. A., Pchelkin, N. R., Wert, J. C., and Mueller, G. W., 1979, "Initial Shock Tube Studies of Monomethylamine," *Journal of Physical Chemistry*, **83**(2), pp. 297-302.
- [48] Yoshihara, Y., and Tanaka, T., 1995, "Reduction of Oxides of Nitrogen in Diesel Exhaust with Addition of Methylamine," *Transactions of JSME (in Japanese), Series B*, **61-582**, pp. 408-413.
- [49] Nakanishi, Y., Tanaka, T., Yoshihara, Y., and Nishiwaki, K., 1999, "Reduction of Nitric Oxide In Diesel Exhaust With the Addition Of Methylamine." *Journal of Engineering for Gas Turbines and Power*, **121**(3), 563-568.
- [50] Nakanishi, Y., Gone, J.D., Yoshihara, Y., and Nishiwaki, K., 2001, "Application of a New Selective Non-Catalytic NO Reduction System to Diesel Exhaust," *Proceedings of the 5th Int Symposium on Diagnostics and Modelling of Combustion in Internal Combustion Engines*, Nagoya, Japan.
- [51] Xu, B. Y., Tian, H. Y., Yang, J., Sun, D. Z., and Cai, S. L., 2011, "A System of Selective Non Catalytic Reduction of NO<sub>x</sub> for Diesel Engine," *Advanced Materials Research*, **201**, pp. 643-646.
- [52] Milewska, A., Hercog, J., and Kakietek, S., 2011, "Experimental investigation of NO<sub>x</sub>reduction using monomethylamine," *11th International Conference on Energy for a Clean Environment*, Lisbon, Portugal.
- [53] Mahmood, A., Hamid, A., Irfan, N., Javed, M. T., and Waheed, K., 2009, "Assessment and Identification of Some Novel NO<sub>x</sub> Reducing Reagents for SNCR Process," *Nucleus*, **46**(3), pp. 205-211.
- [54] *Harzrdous Substance*, 2004, New Jersey Department of Health and Senior Services, Trenton, NJ.

- [55] E. I. du Pont de Nemours and Company, n.d., "Methylamines Technical Information." from [http://www2.dupont.com/Methylamines/en\\_US/tech\\_info/index.html](http://www2.dupont.com/Methylamines/en_US/tech_info/index.html).
- [56] Higashihara, T., Gardiner, W. C., and Hwang, S. M., 1987, "Shock Tube and Modeling Study of Methylamine Thermal Decomposition," *Journal of Physical Chemistry*, **91**(7), pp. 1900-1905.
- [57] Hwang, S. M., Higashihara, T., Gardiner, W. C., and Shin, K. S., 1990, "Shock Tube and Modeling Study of Monomethylamine Oxidation," *Journal of Physical Chemistry*, **94**(7), pp. 2883-2889.
- [58] Coda Zabetta, E., Kilpinen, P., Hupa, M., Ståhl, K., Leppälähti, J., Cannon, M., and Nieminen, J., 2000, "Kinetic Modeling Study on the Potential of Staged Combustion in Gas Turbines for The Reduction of Nitrogen Oxide Emissions from Biomass IGCC Plants," *Energy & fuels*, **14**(4), pp. 751-761.
- [59] Dean, A. M., & Bozzelli, J. W., 2000, "Combustion chemistry of nitrogen," *Gas-phase combustion chemistry*, Springer, New York, pp. 125-341.
- [60] Kantak, M. V., De Manrique, K. S., Aglave, R. H., and Hesketh, R. P., 1997, "Methylamine Oxidation in a Flow Reactor: Mechanism and Modeling," *Combustion and Flame*, **108**(3), pp. 235-265.
- [61] Hjuler, K., Glarborg, P., and Dam-Johansen, K., 1995, "Mutually Promoted Thermal Oxidation of Nitric Oxide and Organic Compounds," *Industrial & engineering chemistry research*, **34**(5), pp. 1882-1888.
- [62] Wikipedia, 2008, "File:Pipe-PFR.svg - Wikipedia, the free encyclopedia," from <http://en.wikipedia.org/wiki/File:Pipe-PFR.svg>.
- [63] Romero, C. E., 1997, "SNCR - CHEMICAL KINETICS COMPUTER MODEL: Development and Documentation," Energy Research Center, Lehigh University, Bethlehem, PA.
- [64] Milewska, A., 2012, Dr. at Institute of Power Engineering - Research Institute, Poland, private communication.
- [65] ICIS Chemical Business, 2006, "CEMICAL PROFILE: Methylamines," from <http://www.icis.com/resources/news/2006/06/16/2014781/chemical-profile-methylamines/>

- [66] TAMINCO people & molecules, 2008, "Price increase amines in North America," from [http://www.taminco.de/component/com\\_customnews/Itemid,667/customnews\\_id,47/](http://www.taminco.de/component/com_customnews/Itemid,667/customnews_id,47/)
- [67] TAMINCO people & molecules, 2013, "Taminco announces price increase for Methylamines and DMF in Europe and North America," from <http://investors.taminco.com/index.php?s=43&item=88>
- [68] Wojichowski, D. L., and Egan, J. T., 2002, "SNCR Reagent Supply Alternatives and Cost Minimization," *Chemical Engineering 2004 - Winning Strategies for Regulatory Compliance and Control Conference*, U.S. Department of Energy of the National Energy Technology Laboratory, Pittsburgh, PA.
- [69] Staudt, J., Kehrer, K., Poczynek, J., Cote, R., Pierce, R., Afonso, R., Slod, A., and Miles, D., 1998, "Optimizing Selective Non-Catalytic Reduction Systems for Cost-Effective Operation on Coal-Fired Electric Utility Boilers," *ICAC Forum '98*.

## **Vita**

The author Yan Qin was born in Guangxi, China in 1988. He went to South China University of Technology to have his undergraduate education in major of Thermal Energy and Power Engineering from 2007 to 2011. During his undergraduate study, he was studying in coal-fired power plant and refrigeration areas. After that, he joined Lehigh University as a graduate student in Mechanical Engineering and he worked closely with Dr. Romero on the project described in this thesis. After the graduation from Department of Mechanical Engineering & Mechanics as a Master of Science, Yan Qin will be a Master of Science student in Computer Engineering in Lehigh University and seeking a career in corresponding area.